Biochemical Journal (2020) **477** 2621–2638
https://doi.org/10.1042/BCJ20200423

PORTLAND PRESS

Research Article

An ATP-responsive metabolic cassette comprised of inositol tris/tetrakisphosphate kinase 1 (ITPK1) and inositol pentakisphosphate 2-kinase (IPK1) buffers diphosphoinositol phosphate levels

Hayley Whitfield[1], Gaye White[1], Colleen Sprigg[1], Andrew M. Riley[2], Barry V.L. Potter[2], Andrew M. Hemmings[1,3] and Charles A. Brearley[1]

[1]School of Biological Sciences, UEA, Norwich Research Park, Norwich NR4 7TJ, U.K.; [2]Medicinal Chemistry and Drug Discovery, Department of Pharmacology, University of Oxford, Mansfield Road, Oxford OX1 3QT, U.K.; [3]School of Chemistry, UEA, Norwich Research Park, Norwich NR4 7TJ, U.K.

Correspondence: Barry V.L. Potter (barry.potter@pharm.ox.ac.uk) or Charles A. Brearley (c.brearley@uea.ac.uk)

Inositol polyphosphates are ubiquitous molecular signals in metazoans, as are their pyrophosphorylated derivatives that bear a so-called 'high-energy' phosphoanhydride bond. A structural rationale is provided for the ability of Arabidopsis inositol tris/tetrakisphosphate kinase 1 to discriminate between symmetric and enantiomeric substrates in the production of diverse symmetric and asymmetric *myo*-inositol phosphate and diphospho-*myo*-inositol phosphate (inositol pyrophosphate) products. Simple tools are applied to chromatographic resolution and detection of known and novel diphosphoinositol phosphates without resort to radiolabeling approaches. It is shown that inositol tris/tetrakisphosphate kinase 1 and inositol pentakisphosphate 2-kinase comprise a reversible metabolic cassette converting Ins(3,4,5,6)P_4 into 5-InsP_7 and back in a nucleotide-dependent manner. Thus, inositol tris/tetrakisphosphate kinase 1 is a nexus of bioenergetics status and inositol polyphosphate/diphosphoinositol phosphate metabolism. As such, it commands a role in plants that evolution has assigned to a different class of enzyme in mammalian cells. The findings and the methods described will enable a full appraisal of the role of diphosphoinositol phosphates in plants and particularly the relative contribution of reversible inositol phosphate hydroxykinase and inositol phosphate phosphokinase activities to plant physiology.

Introduction

Myo-inositol hexakisphosphate (InsP_6) is the predominant form of phosphorus storage molecule in plants, where in storage organs and tissues it may accumulate to several percent of dry weight [1]. The enzymology of InsP_6 synthesis extends to families of enzymes collectively capable of phosphorylating all six hydroxyls of the inositol ring [2]. These include inositol kinase [3] and assorted inositol phosphate (hydroxy) kinases, including inositol 1,3,4-trisphosphate 5/6-kinases, also known as inositol tris/tetrakisphosphate kinases, ITPKs [4–6]; inositol polyphosphate kinases [7], commonly called IPK2 after the yeast ortholog [8] and inositol pentakisphosphate 2-kinases [9], commonly called IPK1, again after the yeast ortholog [8].

ITPK1 controls phosphate homeostasis in Arabidopsis and *Atitpk1* mutants accumulate Ins(3,4,5,6)P_4 and/or its enantiomer [10]. Ins(3,4,5,6)P_4 is also the dominant InsP_4 isomer in *Atipk1* mutants which similarly over-accumulate phosphate [11]. Recently, two groups described phosphoanhydride bond formation on the 5-phosphate of InsP_6 (synthesis of 5-InsP_7, 5-PP-InsP_5) catalyzed by recombinant plant ITPK1 and ITPK2 [12,13]. Others have shown that synthesis of 1,5-InsP_8 (also known as

Received: 21 May 2020
Revised: 29 June 2020
Accepted: 6 July 2020

Accepted Manuscript online: 6 July 2020
Version of Record published: 24 July 2020

Biochemical Journal (2020) 477 2621–2638
https://doi.org/10.1042/BCJ20200423

1,5-bis-PP-InsP$_4$) occurs by 1-phosphorylation of 5-InsP$_7$ and is mediated by VIH1 and VIH2 [14] (see Figure 1). Deletion of Vih1 and Vih2 recapitulates constitutive Pi starvation response [15,16]. These works confirm the identity of plant InsP$_8$ previously described [14,17]. While it seems likely that the ITPK1 contribution to phosphate homeostasis may lie in the provision of the 5-InsP$_7$ precursor of 1,5-InsP$_8$, in yeast 5-InsP$_7$ is the principal agent of activation of the SPX-dependent polyphosphate polymerase VTC [18].

Nevertheless, the question of which PP-InsPs and InsPs competitively control phosphate homeostasis in plants is compounded for many biological and technical reasons: (1) Plants have multiple SPX-domain proteins [19] with potential discrete and/or overlapping functions in phosphate homeostasis and, generally, poorly defined specificity for binding of inositol and diphosphoinositol phosphates. (2) The relative levels of InsP$_7$ and InsP$_8$ species revealed by radiolabeling [10,12,17], InsP$_7$ greater than InsP$_8$, are reversed in recent gel electrophoresis determinations [16]. In the latter study, InsP$_8$ levels are substantially greater than InsP$_7$ in phosphate replete Arabidopsis. (3) The biochemical activities of enzymes such as ITPK1 and VIH1/2 are not fully defined; for VIH1/2, full-length protein has not been studied, while for both ITPK1 and VIH1/2, the reversibility of the hydroxykinase- and phosphokinase functions of these enzymes is not described.

Here, we focus on ITPK1, disruption of which in Arabidopsis has profound effect on InsP$_6$ and InsP$_7$ as well as Ins(3,4,5,6)P$_4$ [10,20]. To study ITPK1, we employ a suite of accessible methodologies that have not previously been applied to diphosphoinositol phosphates. They afford the opportunity to distinguish known and novel diphosphoinositol phosphates and to study the reversibility of enzymes that catalyze their interconversion. The pathways in plants in which ITPK1 participates and those revealed by this study are shown in Figure 1.

Materials and methods

Inositol phosphates

The structures of all inositol phosphates and diphosphoinositol phosphates described in this study are numbered according to the 1D-numbering convention and are shown in Supplementary Figure S1.

InsP$_6$ was obtained from Merck Millipore (Product No. 407125). An acid-hydrolysate of phytate (Sigma P-8810) was prepared and used as chromatographic standard according to Madsen et al. [21]. All InsP$_5$ isomers used as substrate for ITPK1 were obtained from Sichem as decasodium salts. Ins(1,3,4,5,6)P$_5$ obtained from Sichem showed evidence of phosphate migration between *cis*-vicinal hydroxyls. Ins(1,3,4,5,6)P$_5$ used as substrate for IPK1 was synthesized according to published procedures [22] and did not show evidence of phosphate migration. InsP$_4$s and InsP$_3$s were obtained from Cayman Chemical Company or were synthesized according to published procedures [23]. Comparisons made between different enantiomers of enantiomeric pairs were performed with compounds obtained from one source only. Diphosphoinositol phosphates (Supplementary Figure S1): 1-InsP$_7$, 3-InsP$_7$, 5-InsP$_7$ and 5PP-Ins(1,3,4,6)P$_4$ were synthesized similarly to published procedures [24]. 4-InsP$_7$ and 6-InsP$_7$ were synthesized by Dr Henning Jessen, Institute of Organic Chemistry, and the Centre for Integrative Biological Signalling Studies, University of Freiburg, Germany.

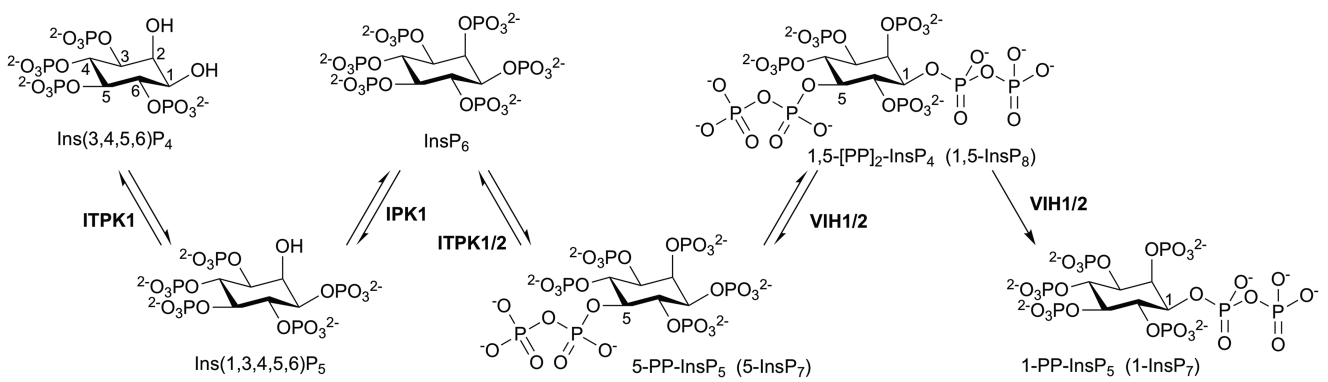

Figure 1. Metabolic relations of inositol phosphates and diphosphoinositol phosphates in plants.

For VIH1/2, the reactions shown have been elucidated only on the separated kinase and phosphatase domains of the protein; for ITPK1 and IPK1, the reversible reactions are the property of a single catalytic domain.

Acid-catalyzed migration of phosphate on ^{32}P-labeled InsPs was performed according to Stephens and Downes [25]. ^{32}P-labeled InsPs were used directly for HPLC without processing to remove nucleotides.

Enzymes: ITPK1

*At*ITPK1 was cloned into the pOPINF plasmid [26], to generate a construct for expression of protein with a 3C cleavable C terminal His tag. Primer sequences used were *5′-AAGTTCTGTTTCAGGGCCCG*ATGTCAGATTC AATCCAGGAAAG-3′ and *5′-ATGGTCTAGAAAGCTTTA*GACATGATTCTTCTTAGTGAC-3′, where the sequence in italics is specific for recombination with the pOPINF vector. Linearized pOPINF plasmid, digested with HindIII and KpnI, was recombined with the PCR product using the In Fusion HD enzyme kit (Clontech) and subsequently transformed into *Escherichia coli* Stellar cells (Clontech). Colonies were confirmed by PCR amplification and transformed into *E. coli* Rosetta 2(DE3)pLysS (Novagen) for protein expression.

ITPK1:His in pOPINF was expressed at 0.1 mM IPTG in Rosetta2 *E. coli* at 18°C overnight and lysed in 25 mM HEPES pH 7.5, 350 mM NaCl, 1 mM DTT, 20 mM imidazole, 1% triton using a French Pressure Cell. Clarified lysate was loaded onto a 5 ml Ni-NTA column (Qiagen) equilibrated in 25 mM HEPES pH 7.5, 350 mM NaCl, 1 mM DTT, 20 mM imidazole and eluted in the same buffer with 20–250 mM imidazole over a 100 ml gradient. The recombinant protein was subsequently purified using a Superdex 75 10/300 column in 20 mM Tris pH7.5, 200 mM NaCl, 2 mM DTT, 10% glycerol, concentrated and stored at −80°C.

IPK1 was prepared according to Whitfield et al. [27] and assayed under the same conditions as ITPK1.

Kinase assays

ITPK1 (typically 0.036 μM, with $InsP_4$; or 33.6 μM, with $InsP_6$) was incubated at 25°C in 10 mM HEPES pH 7.5, 1 mM $MgCl_2$ with 1 mM ATP and 0.5 mM or 1 mM inositol phosphate substrate for periods up 2 h. Assays were typically of 50–100 μl volume.

Kinase assays run under regenerating conditions also contained 5 mM phosphocreatine, 3 U creatine kinase and 1 mM ATP under standard conditions. For ATP K_m calculations ITPK1 was assayed with 0.08–10 mM ATP for 15 min, 40 min or 2 h, depending on the substrate used.

Reactions were terminated by the addition of an equal volume of 60 mM $(NH_4)_2HPO_4$, pH 3.5, with or without incubation at 95°C for 3 min. Samples were clarified by centrifugation at 14 000×***g*** for 5 min and subsequently diluted with an equal volume of deionized water. The injection volume was typically 50 μl.

For incorporation of ^{32}P, assays run in 50 μl volume under ATP-regenerating conditions, 0.5 mM ATP, were supplemented with 10 kBq of [γ-^{32}P] ATP 3000 Ci mmol^{-1} (NEG 502A, PerkinElmer). Assays were run for 2 h at 25°C and reactions stopped by freezing at –20°C. Typically, 25 μl aliquots of the reaction products were diluted to 100 μl with water and 50 μl injected.

HPLC analyses

HPLC was performed according to Whitfield et al. [27] using either 0.6 M methanesulfonic acid or 0.8 M HCl in buffer reservoirs. Inositol phosphates were detected as ferric complexes by UV detection at 290 nm [28]. In some experiments, a second channel of UV data was collected at 254 nm to detect nucleotides. Inositol phosphates are also detected but with reduced sensitivity at this wavelength.

In some experiments, inositol phosphates were analyzed by strong anion exchange high-performance liquid chromatography using a 4.6 × 235 mm Partisphere (Whatman) SAX column according to Kuo et al. [10]. Inositol phosphates were monitored by incorporation of ^{32}P, detected by Cerenkov counting in a Radiomatic 515 series Flow Detector (Canberra Packard). The detector was set to an integration interval of 12 s, and a second channel of data was collected from a UV detector placed upstream of the radio-detector and set to 254 nm to monitor nucleotides.

For calculation of kinetic parameters, peak areas of inositol phosphates were integrated with ChromNav v.2 (Jasco). For the reproduction of HPLC profiles, data were exported from ChromNav v.1 or v.2 (Jasco) or Flo-One (Canberra Packard) software as *x,y* data and redrawn in GraFit v.7 [29].

Measurement of absorbance spectra of inositol phosphate ferric complexes

UV spectra were measured for Ins(3,4,5,6)P_4 and $InsP_6$ in 0.4 mM ferric nitrate, 0.4 M methanesulfonic acid, 0.67% (w/v) perchloric acid in quartz glass cuvettes.

Biochemical Journal (2020) 477 2621–2638
https://doi.org/10.1042/BCJ20200423

Substrate docking calculations

The ITPK1 from *Entamoeba histolytica* [30] shares 55% sequence identity (60% including conservative substitutions) with the Arabidopsis enzyme when calculated over active site residues alone. For the human enzyme, this rises to 70% identity (80% with conservatively varied substitutions). For this reason, it was decided to build a molecular model for Arabidopsis ITPK1 by reference to the structure of the human enzyme. The amino acid sequence of Arabidopsis ITPK1 (Genbank, At5g16760) was accordingly submitted to Phyre2 [31] and a structural model for the enzyme built by reference to PDB ID: 2QB5 (Crystal Structure of Human Inositol 1,3,4-Trisphosphate 5/6-Kinase (ITPK1) in Complex with ADP and Mn^{2+}). Regularization of polypeptide geometry was carried out using Coot [32] where necessary. The final model contained ATP and two magnesium ions. Docking of experimentally verified inositol phosphate substrates (Supplementary Table S1) was carried out using Autodock Vina [33]. A fully flexible model for the ligand and fixed model for the receptor were employed. From the energy-ranked docked conformations (poses) calculated for each substrate, the best 'productive' pose was selected on the basis of (i) lowest energy and (ii) positioning of the acceptor site for hydroxykinase (oxygen) or phosphokinase (phosphorus) activity within a maximum of 3.8 Å of the γ-phosphate phosphorus atom of ATP. The cutoff distance of 3.8 Å was chosen to reflect the fact that a rigid model for the protein was employed in the calculation. Productive poses are those that are reasoned to most likely lead to phosphorylation. Poses were rendered in PyMOL (The PyMOL Molecular Graphics System, Schrödinger, LLC.). Docking data and models are provided as Supplemental Information.

Accession Numbers Sequences corresponding to the subjects of this study can be found in the GenBank/EMBL databases under the following accession numbers: ITPK1 (At5g16760), IPK1 (At5g42810).

Results

We employed anion exchange chromatography on an acid- and hydroxide-stable quaternary amine-functionalized latex (CarboPac PA200, Dionex) as we have done before [27]. This chemistry allows the use of the widest range of eluents. The use of acid allows detection by post-column complexation of inositol phosphate with ferric ion (in acid conditions) and detection of the ferric complex at 290 nm [28]. While the original literature does not explain the physicochemical basis of the absorbance, we may assume from its magnitude (we measured an extinction coefficient of ca. 3200 M^{-1} cm^{-1} for the complex with $InsP_6$) that the absorbance at 290 nm arises from charge transfer transitions, i.e. ligand-field splitting effects of inositol phosphate disturbing symmetry of the octahedral geometry of hexa-co-ordinate hydrated ferric ion [34]. Moreover, while this is a method of choice for analysis of inositol phosphates in animal feed digestive situations where inositol phosphates are abundant [35], we consider that the sensitivity of the method is not widely appreciated for other purposes.

We used both methanesulfonic acid and HCl as eluents. Separations with HCl of $InsP_6$, 5-$InsP_7$, 1-$InsP_7$ and 4-$InsP_7$ are shown (Figure 2A) and of $InsP_6$, 3-$InsP_7$ and 6-$InsP_7$ (Figure 2B). Enantiomeric pairs, 1-$InsP_7$/3-$InsP_7$ and 4-$InsP_7$/6-$InsP_7$ co-eluted (cf. Figure 2A and B), distinct from the *meso*-compound 5-$InsP_7$, well resolved from 5-PP-Ins(1,3,4,6)P_4 which eluted earlier, shortly after $InsP_6$ (Figure 2C). The peaks shown represent injections of ca. 1–2 nmol of compound. The 4-$InsP_7$ and 6-$InsP_7$ samples available to us showed the presence of some $InsP_6$ impurities. The absorbance spectra of Ins(1,4,5,6)P_4 and $InsP_6$ complexes of ferric ion, are shown (Figure 2D). A calibration curve of detector response for $InsP_6$ is shown for methanesulfonic acid eluent, which gives a flatter baseline, in Supplementary Figure S2. The method is sensitive enough for detection of ca. 50 pmol of $InsP_6$ on-column in our hands, but methanesulfonic acid at this concentration did not elute diphosphoinositol phosphates. In measurements of the kinetic parameters of ITPK1 reported later in this manuscript we observed approximately equivalent peak areas for $InsP_6$ and 5-$InsP_7$ eluted with the stronger acid HCl. The estimations are explained at that juncture.

The opportunity to resolve and measure diphosphoinositol phosphates beside 'lower' inositol phosphates without the use of radiolabel is an advance on separations on Partisphere SAX columns, whose silica-based chemistry is not stable under the acid conditions required of post-column complexation with ferric ion. The use of UV detection further allows sampling of data at rates (typically up to 100 Hz) offering resolution beyond fraction collection and scintillation counting, as exemplified [14,36], and beyond on-line radioactivity counting [2]. The method is more convenient and ca. 50–100-fold more sensitive than ^{31}P-NMR (as used to verify the $InsP_6$ kinase activity of ITPK1, Figure 2, [12]). In our hands, the method is several-fold less sensitive than the metal dye detection-HPLC method of Mayr [37] and is much less compromised by the baseline changes that

Biochemical Journal (2020) **477** 2621–2638
https://doi.org/10.1042/BCJ20200423

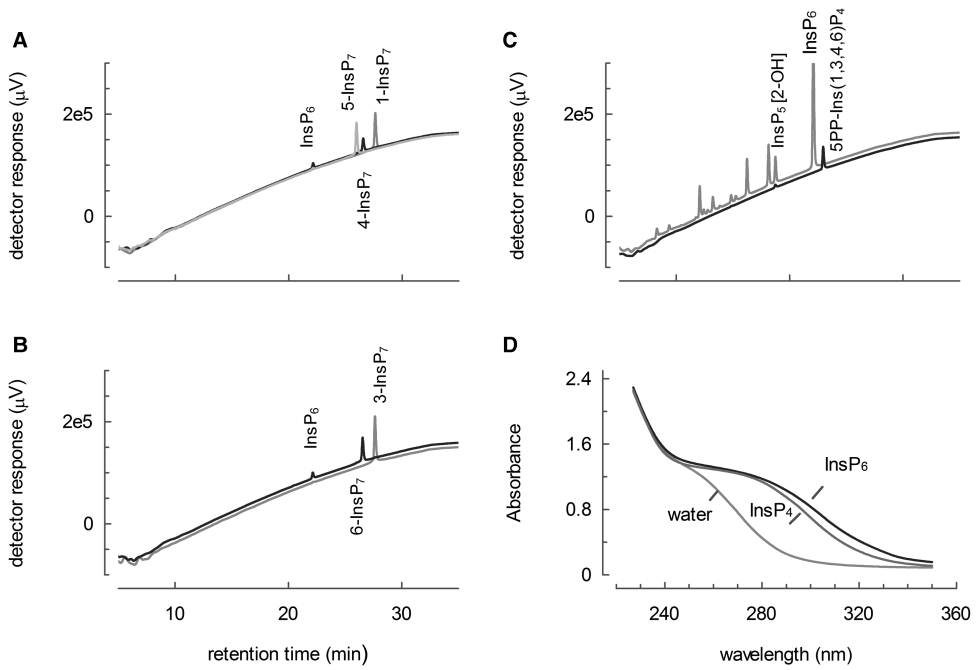

Figure 2. Separations of inositol phosphates and diphosphoinositol phosphates on CarboPac PA200 eluted with HCl.
(**A**) $InsP_6$, black line; 1-$InsP_7$, dark gray line; 5-IP_7, light gray line and 4-$InsP_7$, black line; (**B**) $InsP_6$, black line; 3-$InsP_7$, dark gray line and 6-$InsP_7$, black line; (**C**) an acid-hydrolysate of $InsP_6$, with $InsP_6$ and Ins(1,3,4,5,6)P_5 ($InsP_5$ [2-OH]) labeled, dark gray line; and 5-PP-Ins(1,3,4,6)P_4, black line; (**D**) absorbance spectra of ferric $HClO_4$ (aq) complexes with $InsP_6$, black line; Ins (1,4,5,6)P_4, dark gray line and water, gray line. These experiments have been repeated more than three times with similar results. The structures of compounds described are shown in Supplementary Figure S1.

we have observed of gradients capable of resolving $InsP_2$ through to $InsP_7$ using that method. Moreover, the method we use requires minimal sample preparation as shown for complex animal digesta matrices [35] and, as we show in the following, can be combined with UV detection at wavelengths allowing simultaneous measurement of nucleotides to follow the reversibility of kinase reactions.

We used these methods to examine the substrate specificity of Arabidopsis ITPK1, which belongs to a class of enzyme that has been shown to possess 1-, 5- and 6-hydroxykinase and ($InsP_6$) 5-phosphokinase activities. The availability of pairs of enantiomeric substrates, not available in the radiolabeled form, beside *meso*-compounds, allowed analysis of the enantiospecificity of the enzyme. Of particular interest to us were $InsP_4$ substrates, since Ins(3,4,5,6)P_4 is elevated in *itpk1* and *ipk1* mutants that share a common misregulation of phosphate homeostasis [10,11,38] attributed to deregulated diphosphoinositol phosphate synthesis [15,16]. Of the enantiomeric pairs Ins(1,2,4,6)P_4/Ins(2,3,4,6)P_4, Ins(1,3,4,5)P_4/Ins(1,3,5,6)P_4 and Ins(1,4,5,6)P_4/Ins(3,4,5,6)P_4 (all shown in Supplementary Figure S1), only the latter pair were substrates under ATP-regenerating conditions. The enantiomers were phosphorylated on the 3- and 1-positions, respectively (Figure 3A–H). The activity was robust for both enantiomers, but with much greater activity for Ins(3,4,5,6)P_4 (Figure 3F). The *meso*-isomer Ins(1,3,4,6)P_4, a canonical substrate of phosphoisomerase activity of *Eh*ITPK1and human ITPK1 [30] was not a substrate for hydroxykinase or phosphoisomerase activity (Figure 3G), consistent also with the lack of Ins (1,3,4,5)P_4 hydroxykinase or phosphoisomerase activity (Figure 3C).

We also tested many $InsP_3$ substrates including the enantiomeric pair Ins(1,4,6)P_3/Ins(3,4,6)P_3 (the structures are shown in Supplementary Figure S1 and the HPLC profiles of the reaction products are shown in Supplementary Figure S3A–D). Consistent with the phosphorylation of the enantiomeric pair Ins(1,4,5,6)P_4/Ins (3,4,5,6)P_4, ITPK1 showed phosphorylation of Ins(1,4,6)P_3 at the 3-position and Ins(3,4,6)P_3 at the 1-position. The presence of an Ins(1,3,4,5)P_4 peak for all three $InsP_3$s tested, possibly indicates phosphoisomerase activity at the level of $InsP_4$, under these (non-regenerating for ATP) conditions. The lack of Ins(1,4,5,6)P_4/Ins(3,4,5,6) P_4 product for Ins(1,4,6)P_3 or Ins(3,4,6)P_3 substrates (Supplementary Figure S3B,C) discounts

Biochemical Journal (2020) 477 2621–2638
https://doi.org/10.1042/BCJ20200423

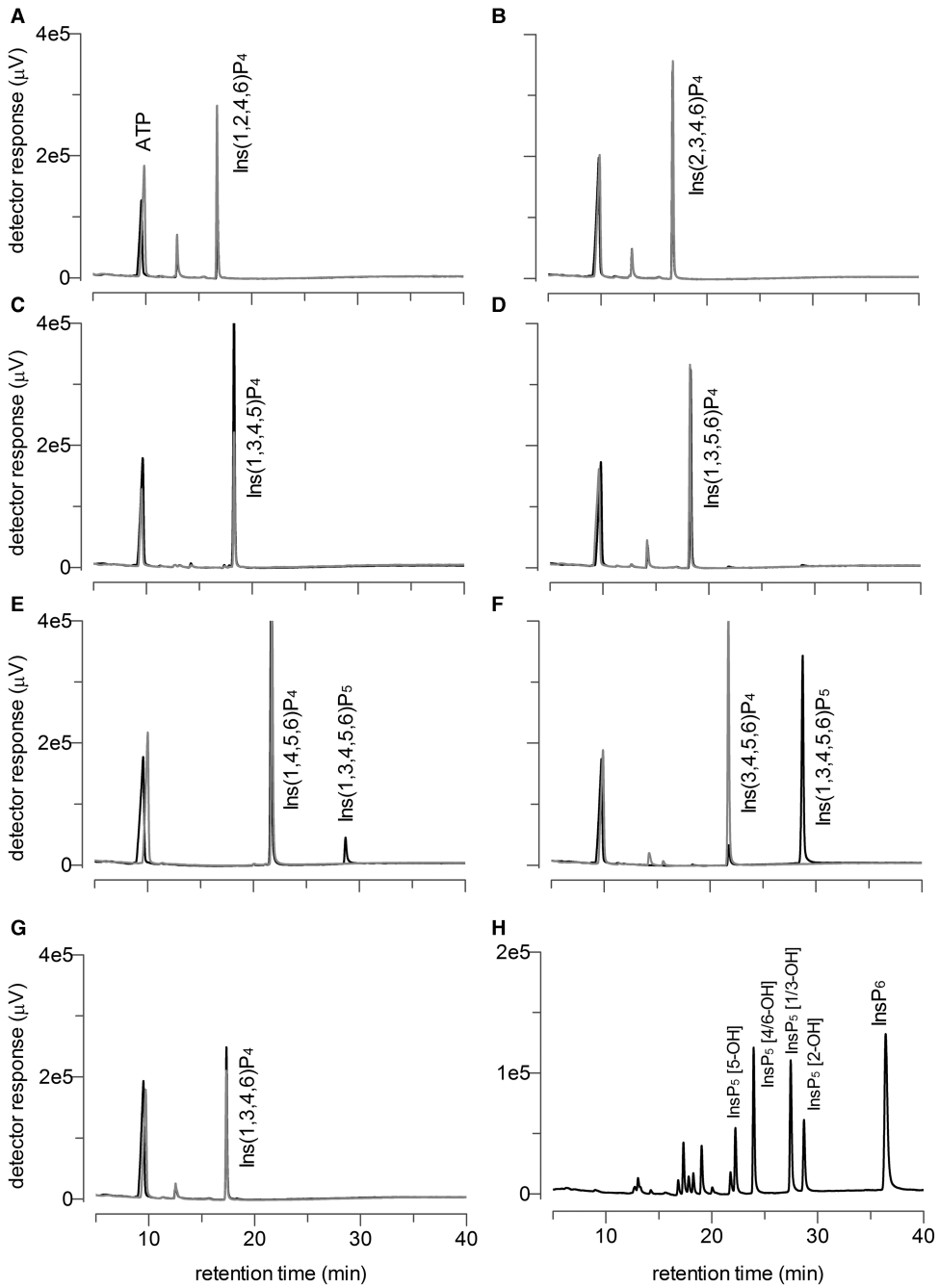

Figure 3. Arabidopsis ITPK1 has robust enantiospecific hydroxykinase activity against Ins(3,4,5,6)P_4.

CarboPac PA200 HPLC analysis of reaction of ITPK1 with (**A**) Ins(1,2,4,6)P_4; (**B**) Ins(2,3,4,6)P_4; (**C**) Ins(1,3,4,5)P_4; (**D**) Ins(1,3,5,6)P_4; (**E**) Ins(1,4,5,6)P_4; (**F**) Ins(3,4,5,6)P_4 and (**G**) Ins(1,3,4,6)P_4; peaks of substrates (ATP and InsP_4) and product (Ins(1,3,4,5,6)P_5) are labeled. Smaller peaks eluting between ATP and InsP_4 are contaminant InsP_3s present in the substrate. Chromatograms in panels (A–G) show a no enzyme control, gray trace, and reaction products, black trace. (**H**) shows elution of an hydrolysate of InsP_6. The HPLC column was eluted with a gradient of methanesulfonic acid. Assays of 50 μl volume were performed in 20 mM HEPES, pH 6.5, 1 mM $MgCl_2$, 1 mM ATP, 0.5 mM InsP_5 in an ATP-regenerating system with 0.036 μM enzyme. These experiments have been repeated more than five times with similar results. The structures of compounds described are shown in Supplementary Figure S1.

5-phosphorylation of these substrates, while the ratio of substrate to product peaks reveals that of the pair, Ins(3,4,6)P_3 is the preferred substrate.

In light of the consistent pattern of phosphorylation of 3- and 1- hydroxyls of Ins(1,4,6)P_3/Ins(1,4,5,6)P_4 and Ins(3,4,6)P_3/Ins(3,4,5,6)P_4 pairs, respectively, we modeled the binding of the enantiomers Ins(1,4,5,6)P_4 and Ins(3,4,5,6)P_4 (to ITPK1 (Figure 4)). We used as reference the specificity subsite nomenclature described for the crystal structure of *E. histolytica* ITPK1 [30]. On this basis our modeling suggests significant interaction of the 4-phosphate of Ins(1,4,5,6)P_4 and of the 6-phosphate of the Ins(3,4,5,6)P_4 in site F (Figure 4A,B). Similarly, we posit that the respective 1- and 3- phosphates of Ins(1,4,5,6)P_4 and Ins(3,4,5,6)P_4 make contacts in site C. Collectively, residues in these subsites are likely determinants of the reactivity of ITPK1. Indeed, K188A mutation abrogates the activity of ITPK1 against $InsP_6$ in *kcs1 vip1 ddp1* yeast, as does D288A mutation [12]. Irrespective of the fine detail, the symmetry-generating capacity of ITPK1's hydroxykinase activity (Supplementary Table S2) suggests fundamental differences in the pose of enantiomeric substrates. We posit that the inositol ring can bind either in 'obverse' (axial 2-OH group facing up and pointing out of active site) as presented for the Ins(1,4,5,6)P_4 (Figure 4A), or 'reverse' (2-OH group face down) orientation as presented for Ins(3,4,5,6)P_4 (Figure 4B).

Because Ins(3,4,5,6)P_4 is a known physiological substrate of human ITPK1 [39], we next compared in more detail the relative activity of ITPK1 for Ins(3,4,5,6)P_4 and the recently identified $InsP_6$ substrate. At low enzyme, $InsP_6$ was not phosphorylated while Ins(3,4,5,6)P_4 was (Figure 5A,B). With 100-fold more enzyme, we confirmed the production of 5-$InsP_7$ from $InsP_6$ (Figure 5C), as reported [12,13]. Because a central tenet of the energy status signaling role of diphosphoinositol phosphates (5-$InsP_7$, specifically) is the high (1–1.2 mM) K_m for ATP of mammalian IP6K [40] and kcs1 [41,42], a more recent estimate for IP6K1 is 0.35 mM [43], we measured kinetic parameters for ATP with these two substrates (Figure 5D,E). Ins(3,4,5,6)P_4 was, by more than two-orders of magnitude (V_{max} 8640 ± 025 nmol min^{-1} mg^{-1} vs 40 ± 3 nmol min^{-1} mg^{-1}), the stronger substrate. The K_m ATP values 1.22 ± 0.37 mM and 0.77 ± 0.19 mM for $InsP_6$ and Ins(3,4,5,6)P_4, respectively, identify both $InsP_6$ and Ins(3,4,5,6)P_4 as metabolites that are responsive to energy status, but the much greater activity towards Ins(3,4,5,6)P_4 focuses attention on this isomer and on historic detailed analyses of inositol phosphate isomerism in plants [2,36,44,45]. Significantly, Ins(3,4,5,6)P_4 was identified in the duckweed *Spirodela polyrhiza* [36], where it is a substrate for phosphorylation by a cytosolic 1-hydroxykinase [2,46]. The pronounced effect of mutation of ITPK1 on phosphate homeostasis [10] gives physiological context to this activity.

To estimate the sensitivity of the method for detection of diphosphoinositol phosphates, we took advantage of the characterized $InsP_6$ kinase activity of ITPK1 to synthesize 5-$InsP_7$ from the readily available precursor $InsP_6$. We note that the lack of commercial availability of diphosphoinositol phosphates does not allow easy comparison of the chemical stability or purity of different diphosphoinositol phosphates between laboratories,

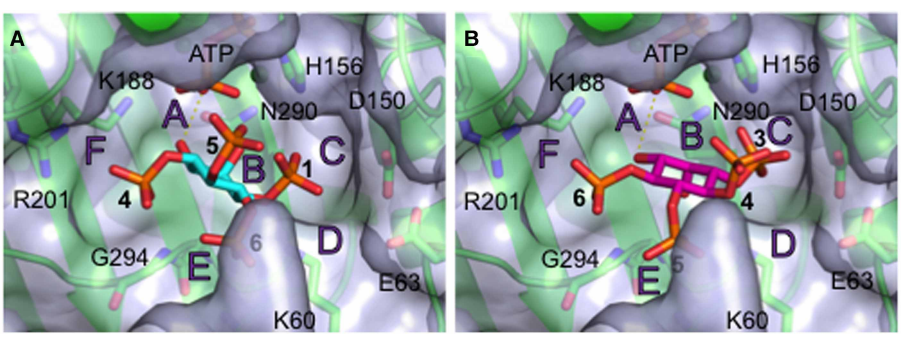

Figure 4. A structural model for enantiospecific kinase activity of *At*ITPK1 towards $InsP_4$ substrates.

Molecular docking-derived models of the complexes of ITPK1 with ATP/Mg^{2+} and Ins(1,4,5,6)P_4 (**A**) and Ins(3,4,5,6)P_4 (**B**). A cartoon representation of ITPK1 is shown in green along with stick representations of ATP and selected active site residues (labeled). The ITPK1 molecular surface is shown in gray. Magnesium ions (partially obscured) are shown as dark green spheres. The distances of closest approach of the γ-phosphate phosphorus of ATP and receiving hydroxyl oxygen (indicated by yellow dashed lines) are less than 3.8 Å in both cases. Specificity subsites as described by Miller et al. [30] are indicated by capital letters (A–F) in each panel. The structures of compounds described are shown in Supplementary Figure S1.

Biochemical Journal (2020) **477** 2621–2638
https://doi.org/10.1042/BCJ20200423

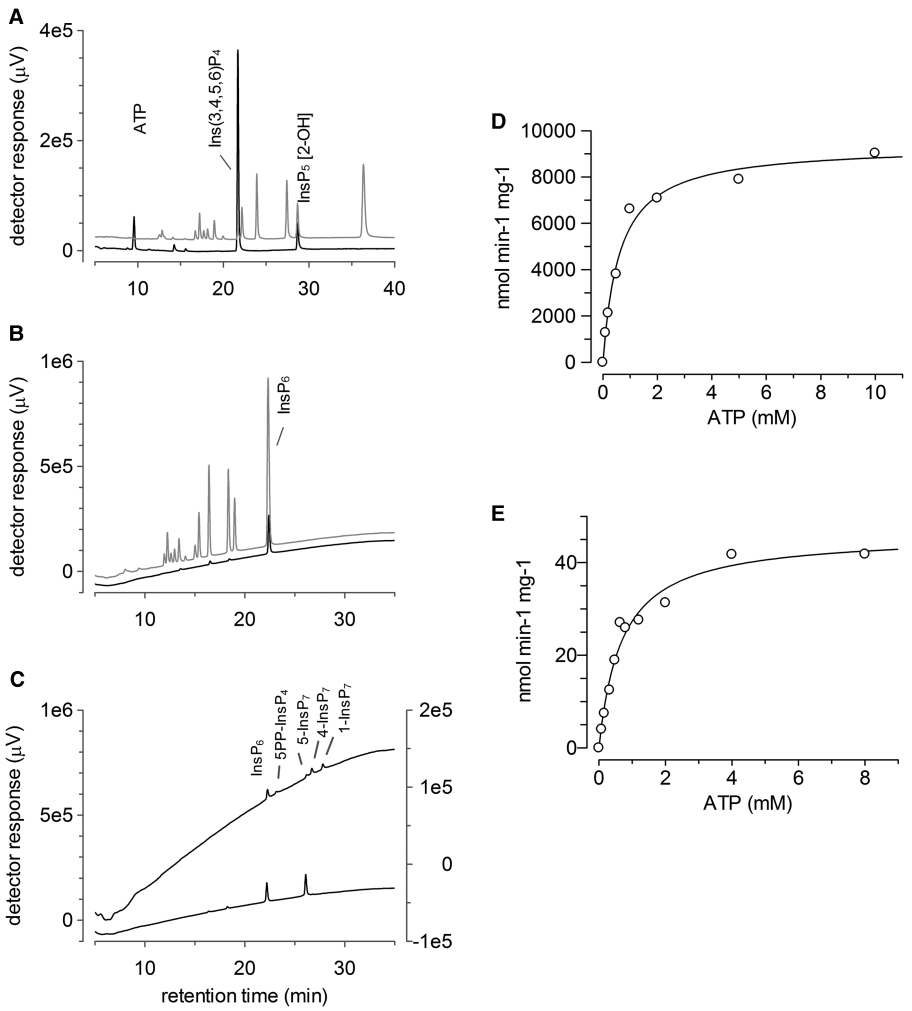

Figure 5. Comparison of Ins(3,4,5,6)P_4 and $InsP_6$ as substrates of Arabidopsis ITPK1.

Products of reaction with Ins(3,4,5,6)P_4 were analyzed with a methanesulfonic acid gradient (**A**), while products of reaction with $InsP_6$ under the same conditions were analyzed with an HCl gradient (**B**); (**C**), as (B) with 100-fold more enzyme. For (A,B), an acid-hydrolysate of $InsP_6$ (different amounts) is shown in gray, shifted on the *Y*-axis to aid visualization. For (C), authentic diphosphoinositol phosphates standards are shown in the upper trace (right *Y*-axis). These experiments have been repeated more than five times with similar results. (**D**) Kinetic analysis with Ins(3,4,5,6)P_4; (**E**) kinetic analysis with $InsP_6$; conversion of substrate to product calculated from integrated HPLC peaks. (D,E) data fitted to the Michaelis–Menten equation, each data point is a single measurement from a single experiment. The experiment was repeated three times. K_m and V_{max} (mean and SD) are given in the text. There was a change in eluent batch between runs shown in (A,B) that accounts for the slight shift in retention times. Assays of 50 μl volume were performed in 20 mM HEPES, pH 7.5, 1 mM $MgCl_2$, 1 mM ATP, 0.5 mM inositol phosphate in an ATP-regenerating system with 0.036 μM enzyme (A,B,D) or 3.6 μM enzyme and 1 mM substrate. (**E**) Assays with Ins(3,4,5,6)P_4 were run typically for 20 min, those with $InsP_6$ for 40–120 min. The structures of compounds described are shown in Supplementary Figure S1.

or their batch-to-batch variation, particularly given the difficulty in separation, detection and quantification. Consequently, we set up an assay with sufficient enzyme to effect the substantive conversion of $InsP_6$. The data (Supplementary Figure S4A–C) show that for HPLC runs from assays with constant starting $InsP_6$, the sum of the integrated peak areas for substrate and product ($InsP_6$ + $InsP_7$) did not vary substantially despite greater than 50% reduction in $InsP_6$ peak area. Thus, we conclude that the sensitivity of the detection of $InsP_6$ and 5-$InsP_7$ is very similar. Moreover, an example chromatogram (Supplementary Figure S4D) shows that with ease it is possible to detect 5-$InsP_7$ at 1% conversion in an assay where approximately one-quarter of the assay

products from a 50 μl assay with 1mM $InsP_6$ were applied to the column (ca. 125 pmol). Close inspection of the baseline (see inset) makes apparent that the sensitivity of the method is rather better than this, probably approaching 20 pmol. For the purpose of illustrating the utility of our methods for *in vivo* measurements, Supplementary Figure S5 shows example chromatograms from the seeds of Arabidopsis wild type, *ipk1-1* and *mrp5-2* mutants (lines described [10]) and Supplementary Figure S6 shows example chromatograms of $InsP_6$ fractions purified from maize and rice bran [21].

We also tested whether ITPK1 has activity against Ins(1,3,4,5,6)P_5 (for structures of $InsP_5$s see Supplementary Figure S1). The data of Figure 6 show that Ins(1,3,4,5,6)P_5 ($InsP_5$ [2-OH]), unlike its metabolic neighbors, Ins(3,4,5,6)P_4 and $InsP_6$ [2], is not a substrate. We point out that the particular substrate obtained from Sichem had almost equimolar $InsP_5$ [2-OH] and $InsP_5$ [1/3-OH] (Figure 6B). The lack of enzymatic product with $InsP_5$ [2-OH]/[1/3-OH] is consistent with the lack of secondary products from Ins(1,4,5,6)P_4 and Ins(3,4,5,6)P_4] (Figure 3). We suggest that Ins(1,3,4,5,6)P_5 binds in the same mode as Ins(3,4,5,6)P_4, but that the axial 2-OH is inappropriately oriented for phosphorylation. Were it to adopt the pose of $InsP_6$, we would expect to see a 5-PP-Ins(1,3,4,6)P_4 product (structure shown in Supplementary Figure S1) which elutes after $InsP_6$ (Figure 2). The lack of this activity distinguishes ITPK1 from kcs1 [47] and IP6K, as noted [13].

Ins(1,3,4,5,6)P_5 is, however, not the only $InsP_5$ present in plants, multiple peaks of $InsP_5$ have been detected by radiolabeling [2,11,14,36,44,45] and in some cases enantiomers resolved. Because Partisphere SAX columns do not adequately resolve Ins(1,2,3,4,6)P_5, from Ins(2,3,4,5,6)P_5 or its enantiomer Ins(1,2,4,5,6)P_5 [2,36,44,45], we tested the ability of ITPK1 to phosphorylate all isomers of $InsP_5$ on the CarboPac PA200 column.

$InsP_5$ isomers bearing a hydroxyl on the 1-, 2-, 3-, 4- and 5-positions (see Supplementary Figure S1 for structures) were not substrates (Figure 6A–E), but Ins(1,2,3,4,5)P_5 ($InsP_5$ [6-OH]) yielded a novel product that is not $InsP_6$ (cf. Figure 6F–G). Given the elution between $InsP_5$s and $InsP_6$, the most parsimonious explanation is that the product is a novel PP-$InsP_4$. We suggest 5-PP-Ins(1,2,3,4)P_4 (structure shown in Supplementary Figure S1), partly on consideration that neither of Ins(1,2,3,5,6)P_5 or Ins(1,2,3,4,5)P_5, nor any of the other $InsP_5$ isomers, are phosphorylated on the vacant hydroxyl (Figure 6A–E), but also on account of the discrete retention time, distinct from 5-PP-Ins(1,3,4,6)P_4 (cf. Figure 2C). We summarize the inositol phosphate hydroxykinase and inositol phosphate phosphokinase reactions catalyzed by ITPK1 in Supplementary Table S2 and present speculative binding modes for Ins(1,2,3,4,5)P_5 and $InsP_6$ to ITPK1 in Figure 7A,B.

The two ligands adopt similar poses in their predicted low energy complexes: binding modes quite dissimilar to those seen for $InsP_3$ or $InsP_4$ ligands. Specifically, for $InsP_6$, the axial 2-phosphate occupies site C and equatorial 3-phosphate site B of the canonical specificity subsite set described by Miller et al. [30]. However, for both Ins(1,2,3,4,5)P_5 and $InsP_6$ ligands the inositol ring rotates to lie roughly perpendicular to that seen for docked $InsP_3$ and $InsP_4$ ligands and the 4-phosphate consequently occupies site E. This forces the 5-phosphate to occupy site A, the site of phosphotransfer. The 1- and 6-phosphates (where they exist) occupy new sites which we name D′ and F′, respectively. Subsite D′ involves residues Asp63, Asp150 and His156, whilst F′ involves His156 and Ser225. These predicted subsites presumably play a role in helping to ameliorate the problems arising from the need to accommodate the steric bulk and phosphate crowding of these substrates.

The commercial unavailability of PP-InsPs, especially PP-$InsP_4$s for which there are 30 theoretical possibilities, five for each $InsP_5$ 'parent', does not allow facile identification of the novel ITPK1 product on chromatographic grounds. The near micromole quantities required for NMR analysis preclude easy confirmation of identity.

Nevertheless, the identification of predominant Ins(3,4,5,6)P_4 1-hydroxykinase activity for ITPK1 affords explanation of *itpk1* phenotype (disruption of $InsP_6$ synthesis and accumulation of Ins(3,4,5,6)P_4 [10,20]). Because ITPK1 and IPK1 individually control phosphate homeostasis, individually accumulate Ins(3,4,5,6)P_4 [10,11,38] and share substrates and products, we next tested whether ITPK1 and IPK1 constitute an ATP-responsive metabolic cassette linking Ins(3,4,5,6)P_4 to 5-$InsP_7$. We combined the two enzymes with nucleotide and Ins(3,4,5,6)P_4. We added equimolar ITPK1 and IPK1 and either buffered ATP with an ATP-regenerating system (this maintains high ATP: ADP ratio) or excluded the ATP-regenerating system, varying ATP: ADP ratio.

In the ATP-regenerating system with 0.1 mM ATP, Ins(3,4,5,6)P_4 was converted via Ins(1,3,4,5,6)P_5 to $InsP_6$ (Figure 8A) and at 1 mM ATP in the regenerating system to 5-$InsP_7$ (Figure 8B). Without the regenerating system, but with 20 : 1 ATP: ADP ratio, Ins(3,4,5,6)P_4 was robustly converted via Ins(1,3,4,5,6)P_5 to $InsP_6$ (Figure 8C), while $InsP_6$ was not significantly phosphorylated (Figure 8D). These experiments show that combination of ITPK1 and IPK1 drives 5-$InsP_7$ synthesis from Ins(3,4,5,6)P_4 in an ATP-dependent manner.

Biochemical Journal (2020) **477** 2621–2638
https://doi.org/10.1042/BCJ20200423

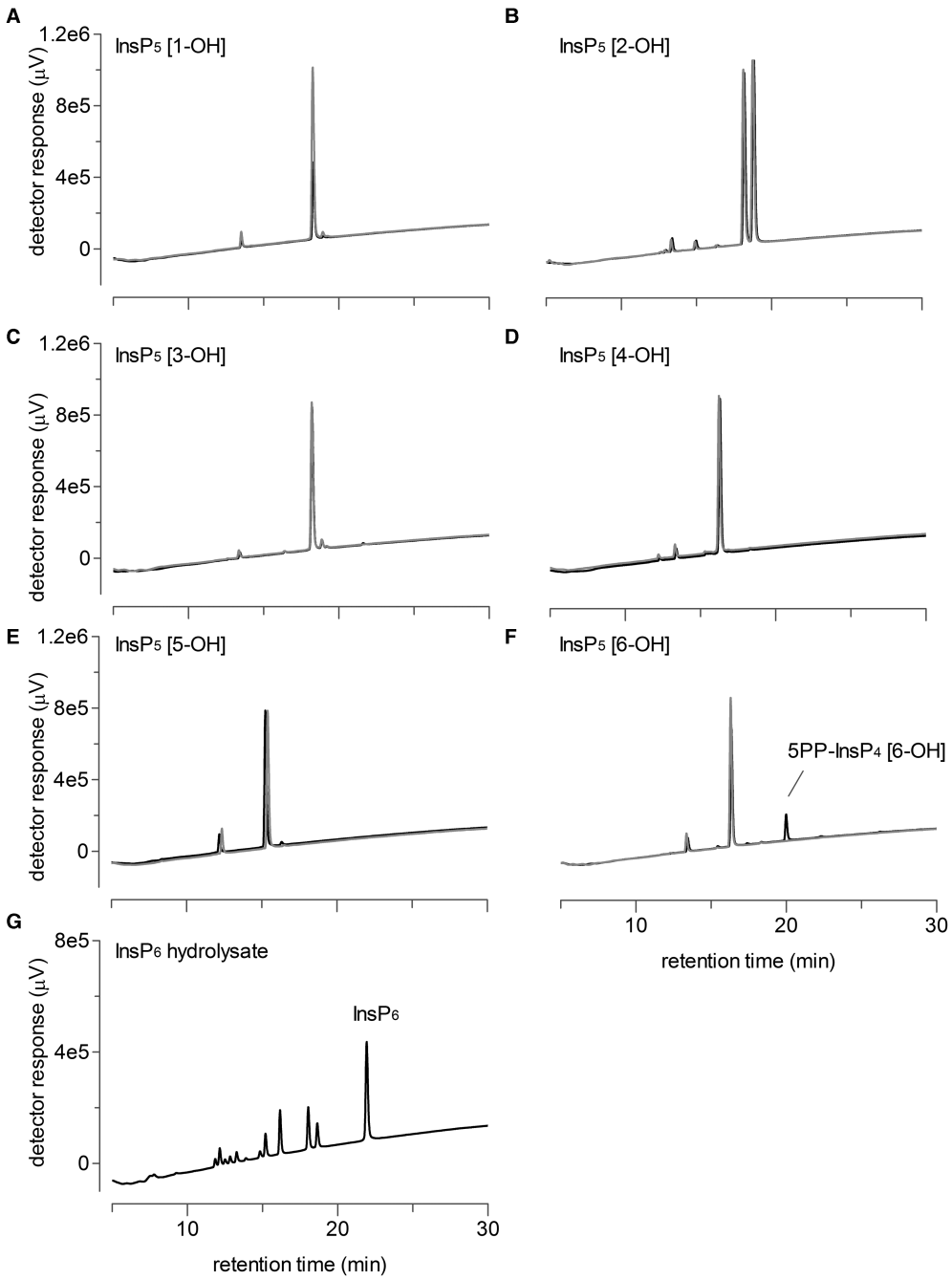

Figure 6. Arabidopsis ITPK1 shows enantiospecific phosphokinase activity on $InsP_5$.

CarboPac PA200 HPLC analysis of reaction products of ITPK1 with (**A**) Ins(2,3,4,5,6)P_5, $InsP_5$ [1-OH]; (**B**) Ins(1,3,4,5,6)P_5, $InsP_5$ [2-OH]; note the commercial product contains near equimolar $InsP_5$ [1/3-OH]; (**C**) Ins(1,2,4,5,6)P_5; $InsP_5$ [3-OH]; (**D**) Ins(1,2,3,5,6)P_5; $InsP_5$ [4-OH]; (**E**) Ins(1,2,3,4,6)P_4, $InsP_5$ [5-OH]; (**F**) Ins(1,2,3,4,5)P_5, $InsP_5$ [6-OH]; (**G**) a set of standards obtained by acid hydrolysis of $InsP_6$ is shown. Chromatograms in panels (A–F) show a no enzyme control, gray trace, and reaction products, black trace. Assays of 50 μl volume were performed in 20 mM HEPES, pH 6.5, 1 mM $MgCl_2$, 1 mM ATP, 0.5 mM $InsP_5$ in an ATP-regenerating system with 0.036 μM enzyme. The HPLC column was eluted with a gradient of HCl. This experiment has been repeated three times with similar results. The structures of compounds described are shown in Supplementary Figure S1.

Biochemical Journal (2020) **477** 2621–2638
https://doi.org/10.1042/BCJ20200423

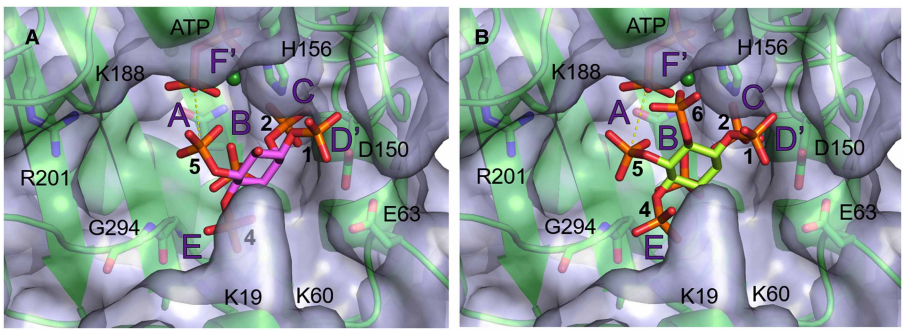

Figure 7. A structural model for phosphokinase activity of ITPK1.

A model of the complex of ITPK1 with Ins(1,2,3,4,5)P_5 and ATP (**A**); a model of the complex of ITPK1 with InsP_6 and ATP (**B**); speculative contacts between the γ phosphate of ATP and the receiving phosphate of the inositol phosphate substrates (indicated by yellow dashed lines) are less than 3.8 Å in both cases. The model was built on the *human* ITPK1 structure (PDB: 2QB5). The structures of compounds described are shown in Supplementary Figure S1.

The reversibility of IPK1 [9,48], kcs1 [41] and IP6K [40,49], led us to test the reversibility of ITPK1. With ITPK1 and IPK1 combined at a 1 : 20 ATP: ADP ratio, InsP_6 was converted via Ins(1,3,4,5,6)P_5 to Ins(3,4,5,6)P_4 and/or Ins(1,4,5,6)P_4 with concomitant generation of ATP (Figure 8E).

At the same nucleotide ratio, ITPK1 generated InsP_6 alone from 5-InsP_7 with the concomitant production of ATP (Figure 9A,B), but was without effect on InsP_6 under the same conditions (Figure 9C,D). The sensitivity of the direction of the reaction catalyzed by ITPK1 to nucleotide ratio is in part similar to IP6K, but unlike for IP6K [49], we did not observe phosphotransfer from IP_6 to ADP, that function is efficiently performed by IPK1 [9,48,50].

By labeling of kinase reaction products with [γ-^{32}P] (see Supplementary Figure S1) and use of more common Partisphere SAX HPLC, we determined the enantiospecificity of ITPK-mediated dephosphorylation of Ins(1,3,4,5,6)P_5. First, we synthesized Ins([^{32}P]1,3,4,5,6)P_5, and Ins(1,[^{32}P]3,4,5,6)P_5, from Ins(3,4,5,6)P_4 and Ins(1,4,5,6)P_4, respectively (Figure 10A,B). Again, we confirmed that Ins(3,4,5,6)P_4 is the much stronger substrate. Next we incubated Ins([^{32}P]1,3,4,5,6)P_5 with ITPK1 at unlabeled nucleotide ratio (ATP:ADP, 1 : 20) favoring phosphotransfer to ADP. We did not observe the production of [^{32}P]InsP_4, despite synthesis of [^{32}P]ATP and an increase in ATP peak area (in the UV_{254} channel). Significantly, the reaction did not generate orthophosphate product (Figure 10C,D). These data show that ITPK1 has a preferential reversible Ins(3,4,5,6)P_4 1-kinase /Ins(1,3,4,5,6)P_5 1-phosphotranferase to ADP (ATP synthase) activity, i.e. the phosphorylation of the preferred enantiomeric (asymmetric) substrate to *meso*- (symmetric) product is reversible in generating the same enantiomer of InsP_4. Using this more common HPLC method we were also able to compare the efficiency of phosphorylation of Ins(3,4,5,6)P_4, Ins(1,2,3,4,5)P_5 and InsP_6 substrates (Figure 10E–G). Ins(3,4,5,6)P_4 was, again, much the preferred substrate, with Ins(1,2,3,4,5)P_5 a slightly weaker substrate than InsP_6. In Supplementary Figure S7, we show that the presumed 5-PP-Ins(1,2,3,4)P_4 product of phosphorylation of Ins(1,2,3,4,5)P_5 elutes between Ins(2,3,4,5,6)P_5 (InsP_5 [1-OH]) and InsP_6 on Partisphere SAX HPLC.

Discussion

Despite historic description of inositol phosphates more highly charged than InsP_6 in amoeboid organisms [51,52], animals [53,54] and plants [44,55,56], the identity of inositol phosphate kinases in plants capable of forming phosphoanhydride bonds has until recently proved enigmatic [12,13]. Because diphosphoinositol phosphates have garnered attention as a cellular signal of eukaryotic energy status, reviewed [42,57,58], the recent works [12,13] focus attention on 5-InsP_7 as an agent of energy signaling in plants.

By measuring K_m ATP for Arabidopsis ITPK1 we show that diphosphoinositol phosphate synthesis from Ins(3,4,5,6)P_4 is responsive to nucleotide ratio, which taking account of AMP is encapsulated as a metabolic concept in the term energy charge [59]. The low affinity of InsP_6 kinase for ATP [40] is a central tenet of the signaling role of 5-InsP_7. Similarly, the K_m ATP of Arabidopsis ITPK1 (1.2 mM) poises the activity of this enzyme within the estimated physiological range of this nucleotide in the cytosol of plants [60–62]. A logical

Biochemical Journal (2020) **477** 2621–2638
https://doi.org/10.1042/BCJ20200423

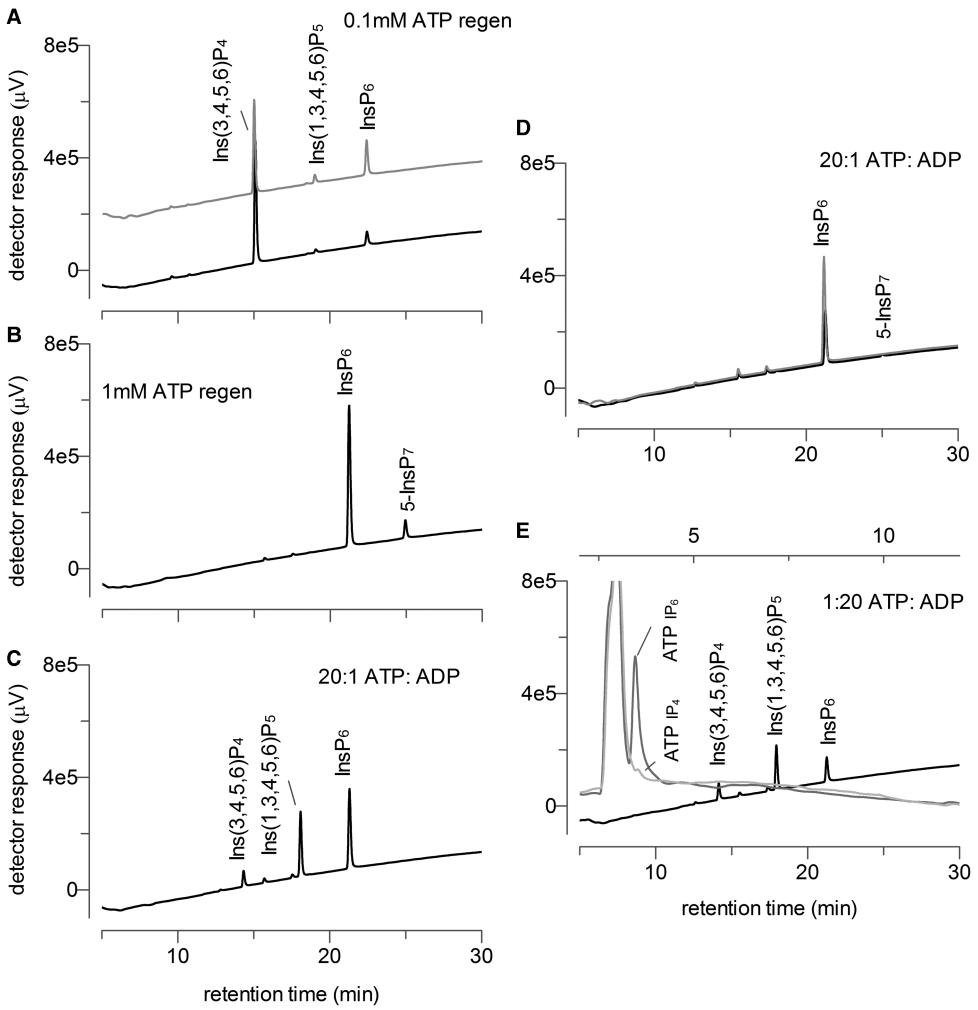

Figure 8. ITPK1 and IPK1 comprise an energy-responsive metabolic cassette. Products of reaction coupled with the two enzymes were analyzed by CarboPac PA200 HPLC.

In an ATP-regenerating system at low ATP, (**A**) Ins(3,4,5,6)P_4 is converted via Ins(1,3,4,5,6)P_5 to InsP_6, 20 min reaction, black line; 40 min reaction, gray line; (**B**) with higher ATP, Ins(3,4,5,6)P_4 is converted via InsP_6 to 5-InsP_7; (**C**) in the absence of the regenerating system and at a 20 : 1 ATP:ADP ratio, Ins(3,4,5,6)P_4 is converted via Ins(1,3,4,5,6)P_5 to InsP_6. For (A–C), the purity of the Ins(3,4,5,6)P_4 substrate used is evidenced in Figure 3F; (**D**) under the same conditions, InsP_6 is not substantially converted to 5-InsP_7, no enzyme control, gray trace; reaction with enzyme, black trace; (**E**) at a 1 : 20 ATP:ADP ratio, InsP_6 is converted via Ins(1,3,4,5,6)P_5 to Ins(3,4,5,6)P_4 with concomitant generation of ATP, the additional traces (time, upper *X*-scale; UV_{254}, *Y*-scale) show generation of an ATP peak when assays are conducted with InsP_6 (dark gray) and the absence of this peak when the same experiment is conducted with Ins(3,4,5,6)P_4 (light gray). Assays of 50 μl or 100 μl volume were performed in 20 mM HEPES, pH 7.5, 1 mM $MgCl_2$, with 0.5 mM Ins(3,4,5,6)P_4 or InsP_6 and an ATP-regenerating system with 0.1 mM ATP (A); 1 mM ATP (B); or without the regenerating system and 5 mM ATP, 0.25 mM ADP (C,D); or 0.25 mM ATP, 5 mM ADP (E). The enzyme concentration was 0.030 μM ITPK1, 0.014 μM IPK1 for (A,B) and 3.6 μM ITPK1, 3.6 μM IPK1 for (C–E). This experiment has been repeated more than three times with similar results; and for (D), the purity of the InsP_6 substrate is evidenced in Figure 5B. The structures of compounds described are shown in Supplementary Figure S1. There was a change in eluent buffer between the experiments shown in (A,B), accounting for the change in the retention time of the InsP_6 peak.

extension is that the physiological levels of all ITPK1 substrates and products, including Ins(3,4,5,6)P_4 and Ins(1,3,4,5,6)P_5, InsP_6 and 5-InsP_7, and for that matter Ins(1,2,3,4,5)P_5 and the presumed 5PP-Ins(1,2,3,4)P_4, are responsive to energy status. Here, by defining the reversibility of ITPK1 we show that the extent and direction of flux between Ins(3,4,5,6)P_4 and 5-InsP_7 is responsive to nucleotide ratio (Figure 1).

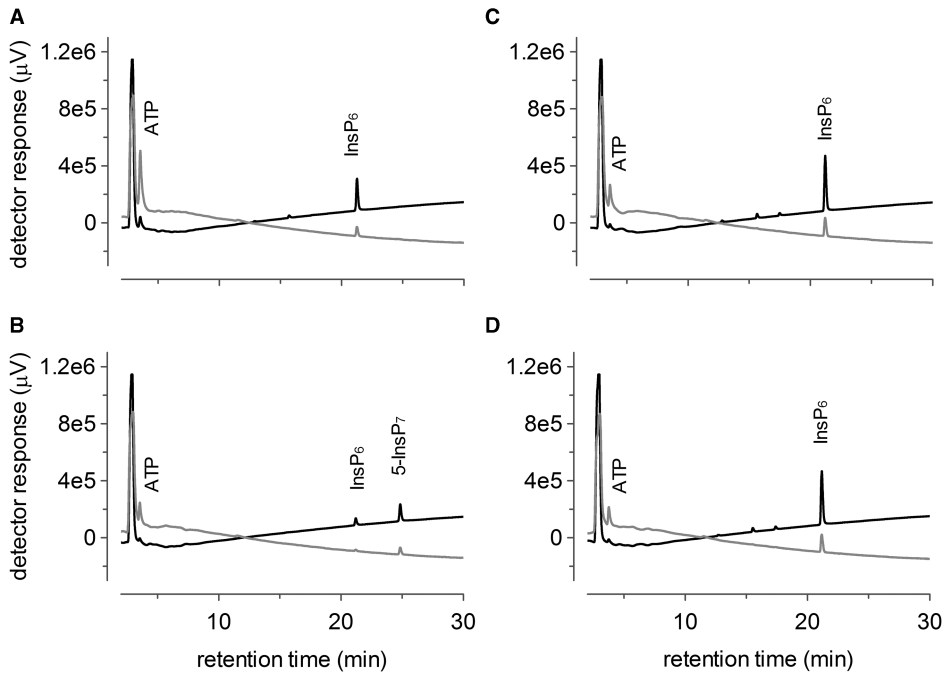

Figure 9. Arabidopsis ITPK1 shows symmetry conserving 5-InsP$_7$-ADP phosphotransferase activity.

CarboPac PA200 HPLC analysis (HCl gradient) of reaction products of ITPK1 with (**A**), 5-InsP$_7$; (**B**) no enzyme control for (A); note conversion of 5-InsP$_7$ to InsP$_6$ (black trace) with concomitant generation of ATP (gray trace, UV$_{254}$); (**C**) InsP$_6$; (**D**) no enzyme control for (C). Assays of 100 μl volume were performed in 20 mM HEPES, pH 7.5, 1 mM MgCl$_2$, 0.25 mM ATP, 5 mM ADP, 0.25 mM 5-InsP$_7$ or 0.5 mM InsP$_6$ with 3.6 μM enzyme for 1 h (A,B) or 3 h (C,D). This experiment has been repeated more than three times with similar results. The structures of compounds described are shown in Supplementary Figure S1.

While 5-InsP$_7$ is a reported regulator of phosphate homeostasis in yeast [63], it has been shown in metazoans, the HCT116 cell line, that both 5-InsP$_7$ and 1,5-InsP$_8$ are responsive to extracellular Pi, but 1,5-InsP$_8$ more so [64]. This is explained in part by inhibition of phosphatase activities of PPIP5K1 and PPIP5K2 by Pi, and activation, for PPIP5K2 of kinase activity.

The plant orthologs of PPIP5K have proved recalcitrant to study as full-length enzymes, but plants bearing deletion of Vih1 and Vih2 show constitutive Pi starvation responses recapitulating itpk1 phenotype [10,15]. The activities of the separated recombinant kinase and phosphatase domains of VIH1 and VIH2 [13–16] are shown (Figure 1). What is not clear is how full-length VIH is influenced by different nucleotides or nucleotide ratio *in vitro* or *in vivo*. Since recombinant full-length ScVip1 converts 5-InsP$_7$ to InsP$_8$ at supra-mM Mg^{2+}-ATP and produces InsP$_6$ at sub-mM Mg^{2+}-ATP [15] we may expect VIH1/2 to do the same, but whether VIH1/2 (or ScVip) show diphosphoinositol phosphate-'driven' ATP synthase activity (from InsP$_7$ or InsP$_8$) in the manner of IP6K and Kcs1 [40,41,49] and *At*ITPK1 (this study) is not resolved. Clearly, the example of *At*ITPK1 illustrates how reversibility of the activity(s) of full-length VIH1/2 is critical to our understanding of phosphate homeostasis, since between them ITPK1 and VIH1/2 set the balance between 5-InsP$_7$ and 1,5-InsP$_8$ as ligands of SPX-domain-containing proteins.

Reversibility of plant inositol phosphate (hydroxyl) kinases is, however, well documented for ITPKs [6,65] and IPK1 [9,48], the latter echoing earlier work on a mung bean activity [50] for which physiological context in germinative ATP synthesis was predicted as early as 1963 [66]. Consideration of these works shows how enzymes such as IPK1 with large equilibrium constants [9] can drive phosphoanhydride formation. Moreover, they show that phosphoanhydride formation is not a priori a facet of 'high-energy' status of either substrate, it can for reversible enzymes merely reflect prevailing substrate concentration.

Considering *At*ITPK1's contribution to InsP and PP-InsP metabolism, Saiardi and co-workers [67] have shown by heterologous expression of ITPK1 orthologs in yeast how inositol phosphate metabolism may be cryptic, or at least hidden to conventional radiolabeling. Without measurement of specific radioactivity of

Biochemical Journal (2020) **477** 2621–2638
https://doi.org/10.1042/BCJ20200423

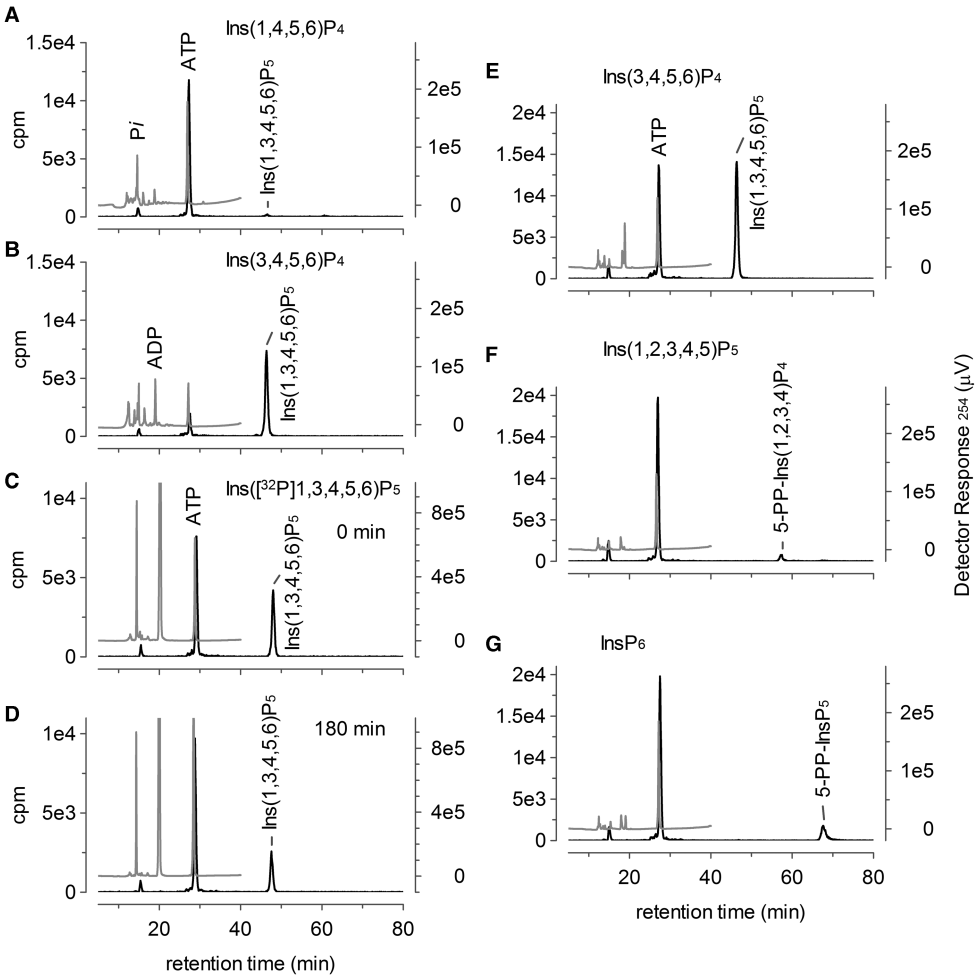

Figure 10. Partisphere SAX HPLC analysis of phosphotransfer reactions catalyzed by ITPK1.

Kinase reaction of ITPK1 with [γ-^{32}P]ATP and (**A**) Ins(1,4,5,6)P_4; (**B**) Ins(3,4,5,6)P_4; ATP synthase reaction of ITPK1 with Ins([^{32}P]1,3,4,5,6)P_5 and ADP (**C**), 0 min; (**D**) 180 min. Comparison of kinase reaction of ITPK1 with Ins(3,4,5,6)P_4 (**E**); Ins(1,2,3,4,5)P_5 (**F**) and $InsP_6$ (**G**). (A–G) Left *Y*-axis, cpm, black lines; right *Y*-axis, gray trace, UV_{254}. All panels show the presence of unconsumed ATP in the assay products. For (D), there is an enzyme-dependent increase in ATP at the expense of Ins([^{32}P]1,3,4,5,6)P_5. Assays in the kinase direction were performed under ATP-regenerating conditions with 1 mM ATP, 0.25 mM inositol phosphate and 0.036 μM enzyme for 1 h (A,B). A separate assay run for 3 h is shown (E–G). Assays in (C,D) were performed with 0.25 mM ATP, 5 mM ADP for 2 h. The structures of compounds described are shown in Supplementary Figure S1.

metabolite pools, labeling studies run the risk of missing these 'cryptic' pathways. The work of Stephens and Downes [25] is a notable exception that remarkably defined a pathway for phosphorylation of Ins(3,4,6)P_3 via Ins(3,4,5,6)P_5 to Ins(1,3,4,5,6)P_5 that is paralleled in duckweed [2,36,46]. Given the identification of $InsP_7$ and $InsP_8$ in duckweed [55], it is likely that $InsP_8$ synthesis therein is catalyzed through the contribution of orthologs of *At*ITPK1 and *At*IPK1 whose reversible nature in 5-$InsP_7$ synthesis/turnover is revealed here (Figure 1).

Moreover, our analysis suggests that ITPK1's substantially greater activity for Ins(3,4,5,6)P_4 over $InsP_6$, coupled through IPK1, is 'matched' to the different pool sizes of Ins(3,4,5,6)P_4 and $InsP_6$ [10]. Indeed, $InsP_6$ is typically two orders of magnitude more strongly labeled, but not in vegetative duckweed [2,36]. While we caution again of the limitations of radiolabeling without independent measurement of pool size, such a proposition explains well the phenotype of *itpk1* mutants, viz. increase in Ins(3,4,5,6)P_4 and decrease in 5-$InsP_7$.

Most interestingly, perhaps, our work reveals how evolution has assigned the same function, an eminently reversible and nucleotide-sensitive $InsP_6$/5-$InsP_7$ phosphotransferase activity, to wholly different enzymes in plants and mammals. ITPK1, and perhaps ITPK2, assume the role of IP6K, or vice-versa, despite the presence

of ITPK1 homolog in mammals. This places special emphasis on ITPK1. As we have shown, *itpk1* mutants make less $InsP_6$, $InsP_7$ and, most likely, $InsP_8$, and hyperaccumulate phosphate [10]. Others [15,16] have collectively assigned special function to $InsP_8$ as the cognate binding partner for SPX1 which interacts with the master transcriptional regulator, PHR1, of phosphate starvation responses. Consistent with studies in barley leaves [68], we have previously shown a shoot-specific near doubling in ATP levels on phosphate starvation. This increase, also in ATP/AMP ratio, was associated with a shoot-specific increase in $InsP_7$. This is consistent with the nucleotide ratio-dependent control of ITPK1 that we demonstrate here. Others, however, have reported that whole seedlings starved of phosphate, and hence showing full phosphate starvation responses, increase nucleotides and ATP/ADP ratio approximately 2-fold on re-supply of phosphate [15].

Of course, plants are photosynthetic autotrophs, which yeast and mammals are not. Plants couple phosphate import across the chloroplast membrane to export of triose phosphate for growth, in an obligatory manner. These points caution that there are substantive differences in phosphate homeostasis between eukaryotes, extending to the engagement of multiple SPX-domain proteins in plants [19]. Just as there are substantive differences in the fundaments of phosphoinositide signaling between plants, animals and yeast we may anticipate differences in control of phosphate homeostasis at the level of diphosphoinositol phosphate interaction with SPX proteins. The evolutionary diversification of ITPK [6,10,12,13,65] and SPX [19] families in plants say as much. Significantly, we have shown that ITPK2, despite its $InsP_6$ kinase activity [12,13] does not regulate phosphate starvation responses, nor do ITPK3 and ITPK4 [10]. If plants engage diphosphoinositol phosphates in as wide a range of physiological functions as animal cells, we can expect ITPK1 and ITPK2 to be engaged in other aspects of plant physiology, but for plants — integration with photosynthesis is likely to be critical. Here, tools that allow simultaneous measurement of subcellular nucleotide pools [62] could be brought to bear to elucidate the complex relationships between intracellular phosphate, nucleotides and diphosphoinositol phosphates. Nevertheless, the responsiveness of the direction of ITPK1 activity to the nucleotide ratio is likely a critical control point.

Open access

Open access for this article was enabled by the participation of University of East Anglia in an all-inclusive *Read & Publish* pilot with Portland Press and the Biochemical Society under a transformative agreement with JISC.

Competing Interests

The authors declare that there are no competing interests associated with the manuscript.

Author Contributions

H.W., G.W., C.S., A.M.R., A.M.H. and C.A.B. performed experiments. H.W., A.M.R., B.V.L.P., A.M.H. and C.A.B. designed the study. C.A.B. wrote the manuscript with contributions from all authors.

Funding

Funding supporting this study was obtained by C.A.B. and B.V.L.P. C.S. acknowledges the support of a BBSRC Norwich Research Park Doctoral Training Studentship [grant no. BB/M011216/1] with contribution from AB Vista. B.V.L.P. is a Wellcome Trust Senior Investigator [grant no.101010].

Acknowledgements

We thank Huifen Kuo and Tzyy-Jen Chiou (Agricultural Biotechnology Research Center, Academia Sinica, Taiwan) for helpful discussions of the work, and our reviewers for their comments that have improved the manuscript.

Abbreviations

*At*IPK1, *Arabidopsis thaliana* inositol pentakisphosphate 2-kinase *At*ITPK1, *Arabidopsis thaliana* inositol tris/tetrakisphosphate kinase 1; *Dd*ITPK1, *Dictyostelium discoideum* inositol tris/tetrakisphosphate kinase 1; DTT, reduced dithiothreitol; EDTA, ethylenediamine tetra-acetic acid; HEPES, 4-(2-hydroxyethyl)-1-piperazineethane sulfonic acid; His, histidine; HPLC, high-pressure liquid chromatography; *Hs*ITPK1, *Homo sapiens* inositol tris/tetrakisphosphate kinase 1; IP6K, inositol hexakisphosphate kinase; IPK2, inositol polyphosphate multikinase; $Ins(1,3,4)P_3$, 1D-*myo*-inositol 1,3,4-trisphosphate; $Ins(1,4,6)P_3$, 1D-*myo*-inositol 1,4,6-trisphosphate; $Ins(3,4,6)P_3$, 1D-*myo*-inositol 3,4,6-trisphosphate; $Ins(1,2,4,6)P_3$, 1D-*myo*-inositol 1,2,4,6-tetrakisphosphate; $Ins(1,3,4,6)P_4$,

Biochemical Journal (2020) **477** 2621–2638
https://doi.org/10.1042/BCJ20200423

myo-inositol 1,3,4,6-tetrakisphosphate; Ins(1,4,5,6)P_4, 1D-*myo*-inositol 1,4,5,6-tetrakisphosphate; Ins(1,3,5,6)P_4, 1D-*myo*-inositol 1,3,5,6-tetrakisphosphate; Ins(2,3,4,6)P_4, 1D-*myo*-inositol 2,3,4,6-tetrakisphosphate; Ins(3,4,5,6)P_4, 1D-*myo*-inositol 3,4,5,6-tetrakisphosphate; Ins(1,2,3,4,5)P_5, 1D-*myo*-inositol 1,2,3,4,5-pentakisphosphate; Ins(1,2,3,4,6)P_5, *myo*-inositol 1,2,3,4,6-pentakisphosphate; Ins(1,2,3,5,6)P_5, 1D-*myo*-inositol 1,2,3,5,6-pentakisphosphate; Ins(1,2,4,5,6)P_5, 1D-*myo*-inositol 1,2,4,5,6-pentakisphosphate; Ins(1,3,4,5,6)P_5, *myo*-inositol 1,3,4,5,6-pentakisphosphate; Ins(2,3,5,4,6)P_5, 1D-*myo*-inositol 2,3,4,5,6-pentakisphosphate; InsP_6, Ins(1,2,3,4,5,6)P_6, *myo*-inositol 1,2,3,4,5,6-hexakisphosphate; 5-PP-Ins(1,2,3,4)P_4, 1D-5-diphospho-*myo*-inositol 1,2,3,4-tetrakisphosphate; 5-PP-Ins(1,3,4,6)P_4 5-diphospho-*myo*-inositol 1,3,4,6-tetrakisphosphate;1-InsP_7, 1-PP-InsP_5, 1D-1-diphospho-*myo*-inositol 2,3,4,5,6-pentakisphosphate; 3-InsP_7, 3-PP-InsP_5, 1D-3-diphospho-*myo*-inositol 1,2,4,5,6-pentakisphosphate; 4-InsP_7, 4-PP-InsP_5, 1D-4-diphospho-*myo*-inositol 1,3,5,6-pentakisphosphate; 5-InsP_7, 5-PP-InsP_5, 5-diphospho-*myo*-inositol 1,2,3,4,6-pentakisphosphate; 6-InsP_7, 6-PP-InsP_5, 1D-6-diphospho-*myo*-inositol 1,2,3,4,5-pentakisphosphate; 1,5-InsP_8, 1D-1,5-bis-diphospho-*myo*-inositol 2,3,4,6-tetrakisphosphate; Ni-NTA, nickel-nitriloacetic acid; *Os*ITPK1, *Oryza sativa* inositol tris/tetrakisphosphate kinase 1; PCR, polymerase chain reaction; PHR1, *Arabidopsis* Phosphate Starvation Response 1; PPIP5K, diphosphoinositol pentakisphosphate kinase; SPX1, SYG1/Pho81/XPR1 domain-containing protein 1; Tris, tris(hydroxymethyl)aminomethane; VIH1, *Arabidopsis thaliana* diphosphoinositol pentakisphosphate kinase 1; VIH2, *Arabidopsis thaliana* diphosphoinositol pentakisphosphate kinase 2.

References

1 Raboy, V. (2003) *myo*-Inositol-1,2,3,4,5,6-hexakisphosphate. *Phytochemistry* **64**, 1033–1043 https://doi.org/10.1016/S0031-9422(03)00446-1
2 Brearley, C.A. and Hanke, D.E. (1996) Metabolic evidence for the order of addition of individual phosphate esters in the *myo*-inositol moiety of inositol hexakisphosphate in the duckweed *Spirodela polyrhiza* L. *Biochem. J.* **314**, 227–233 https://doi.org/10.1042/bj3140227
3 Shi, J., Wang, H., Hazebroek, J., Ertl, D.S. and Harp, T. (2005) The maize low-phytic acid 3 encodes a *myo*-inositol kinase that plays a role in phytic acid biosynthesis in developing seeds. *Plant J.* **42**, 708–719 https://doi.org/10.1111/j.1365-313X.2005.02412.x
4 Shi, J., Wang, H., Wu, Y., Hazebroek, J., Meeley, R.B. and Ertl, D.S. (2003) The maize low-phytic acid mutant lpa2 is caused by mutation in an inositol phosphate kinase gene. *Plant Physiol.* **131**, 507–515 https://doi.org/10.1104/pp.014258
5 Wilson, M.P. and Majerus, P.W. (1996) Isolation of inositol 1,3,4-trisphosphate 5/6-kinase, cDNA cloning and expression of the recombinant enzyme. *J. Biol. Chem.* **271**, 11904–11910 https://doi.org/10.1074/jbc.271.20.11904
6 Sweetman, D., Stavridou, I., Johnson, S., Green, P., Caddick, S.E. and Brearley, C.A. (2007) *Arabidopsis thaliana* inositol 1,3,4-trisphosphate 5/6-kinase 4 (AtITPK4) is an outlier to a family of ATP-grasp fold proteins from Arabidopsis. *FEBS Lett.* **581**, 4165–4171 https://doi.org/10.1016/j.febslet.2007.07.046
7 Stevenson-Paulik, J., Odom, A.R. and York, J.D. (2002) Molecular and biochemical characterization of two plant inositol polyphosphate 6-/3-/5-kinases. *J. Biol. Chem.* **277**, 42711–42718 https://doi.org/10.1074/jbc.M209112200
8 York, J.D., Odom, A.R., Murphy, R., Ives, E.B. and Wente, S.R. (1999) A phospholipase C-dependent inositol polyphosphate kinase pathway required for efficient messenger RNA export. *Science* **285**, 96–100 https://doi.org/10.1126/science.285.5424.96
9 Phillippy, B.Q., Ullah, A.H. and Ehrlich, K.C. (1994) Purification and some properties of inositol 1,3,4,5,6-pentakisphosphate 2-kinase from immature soybean seeds. *J. Biol. Chem.* **269**, 28393–28399 PMID:7961779
10 Kuo, H.F., Hsu, Y.Y., Lin, W.C., Chen, K.Y., Munnik, T., Brearley, C.A. et al. (2018) Arabidopsis inositol phosphate kinases, IPK1 and ITPK1, constitute a metabolic pathway in maintaining phosphate homeostasis. *Plant J.* **95**, 613–630 https://doi.org/10.1111/tpj.13974
11 Stevenson-Paulik, J., Bastidas, R.J., Chiou, S.T., Frye, R.A. and York, J.D. (2005) Generation of phytate-free seeds in Arabidopsis through disruption of inositol polyphosphate kinases. *Proc. Natl. Acad. Sci. U.S.A.* **102**, 12612–12617 https://doi.org/10.1073/pnas.0504172102
12 Laha, D., Parvin, N., Hofer, A., Giehl, R.F.H., Fernandez-Rebollo, N., von Wiren, N. et al. (2019) Arabidopsis ITPK1 and ITPK2 have an evolutionarily conserved phytic acid kinase activity. *ACS Chem. Biol.* **14**, 2127–2133 https://doi.org/10.1021/acschembio.9b00423
13 Adepoju, O., Williams, S.P., Craige, B., Cridland, C., Sharpe, A.K.A.M., Brown, A.M. et al. (2019) Inositol trisphosphate kinase and diphosphoinositol pentakisphosphate kinase enzymes constitute the inositol pyrophosphate synthesis pathway in plants. *bioRxiv* https://doi.org/10.1101/724914
14 Desai, M., Rangarajan, P., Donahue, J.L., Williams, S.P., Land, E.S., Mandal, M.K. et al. (2014) Two inositol hexakisphosphate kinases drive inositol pyrophosphate synthesis in plants. *Plant J.* **80**, 642–653 https://doi.org/10.1111/tpj.12669
15 Zhu, J., Lau, K., Puschmann, R., Harmel, R.K., Zhang, Y., Pries, V. et al. (2019) Two bifunctional inositol pyrophosphate kinases/phosphatases control plant phosphate homeostasis. *eLife* **8**, e43582 https://doi.org/10.7554/eLife.43582
16 Dong, J., Ma, G., Sui, L., Wei, M., Satheesh, V., Zhang, R. et al. (2019) Inositol pyrophosphate InsP_8 acts as an intracellular phosphate signal in Arabidopsis. *Mol. Plant.* **12**, 1463–1473 https://doi.org/10.1016/j.molp.2019.08.002
17 Laha, D., Johnen, P., Azevedo, C., Dynowski, M., Weiss, M., Capolicchio, S. et al. (2015) VIH2 regulates the synthesis of inositol pyrophosphate InsP_8 and jasmonate-dependent defenses in Arabidopsis. *Plant Cell* **27**, 1082–1097 https://doi.org/10.1105/tpc.114.135160
18 Gerasimaite, R., Pavlovic, I., Capolicchio, S., Hofer, A., Schmidt, A., Jessen, H.J. et al. (2017) Inositol pyrophosphate specificity of the SPX-dependent polyphosphate polymerase VTC. *ACS Chem. Biol.* **12**, 648–653 https://doi.org/10.1021/acschembio.7b00026
19 Jung, J.Y., Ried, M.K., Hothorn, M. and Poirier, Y. (2018) Control of plant phosphate homeostasis by inositol pyrophosphates and the SPX domain. *Curr. Opin. Biotechnol.* **49**, 156–162 https://doi.org/10.1016/j.copbio.2017.08.012
20 Kim, S.I. and Tai, T.H. (2011) Identification of genes necessary for wild-type levels of seed phytic acid in Arabidopsis thaliana using a reverse genetics approach. *Mol. Genet. Genom.* **286**, 119–133 https://doi.org/10.1007/s00438-011-0631-2

21 Madsen, C.K., Brearley, C.A. and Brinch-Pedersen, H. (2019) Lab-scale preparation and QC of phytase assay substrate from rice bran. *Anal. Biochem.* **578**, 7–12 https://doi.org/10.1016/j.ab.2019.04.021
22 Godage, H.Y., Riley, A.M., Woodman, T.J., Thomas, M.P., Mahon, M.F. and Potter, B.V.L. (2013) Regioselective opening of *myo*-inositol orthoesters: mechanism and synthetic utility. *J. Org. Chem.* **78**, 2275–2288 https://doi.org/10.1021/jo3027774
23 Mills, S.J., Riley, A.M., Liu, C., Mahon, M.F. and Potter, B.V.L. (2003) A definitive synthesis of D-*myo*-inositol 1,4,5,6-tetrakisphosphate and its enantiomer D-*myo*-inositol 3,4,5,6-tetrakisphosphate from a novel butane-2,3-diacetal-protected inositol. *Chem. Eur. J.* **9**, 6207–6214 https://doi.org/10.1002/chem.200305207
24 Wang, H., Godage, H.Y., Riley, A.M., Weaver, J.D., Shears, S.B. and Potter, B.V.L. (2014) Synthetic inositol phosphate analogs reveal that PPIP5K2 has a surface-mounted substrate capture site that is a target for drug discovery. *Chem. Biol.* **21**, 689–699 https://doi.org/10.1016/j.chembiol.2014.03.009
25 Stephens, L.R. and Downes, C.P. (1990) Product-precursor relationships amongst inositol polyphosphates. Incorporation of [^{32}P]Pi into *myo*-inositol 1,3,4,6-tetrakisphosphate, *myo*-inositol 1,3,4,5-tetrakisphosphate, *myo*-inositol 3,4,5,6-tetrakisphosphate and *myo*-inositol 1,3,4,5,6-pentakisphosphate in intact avian erythrocytes. *Biochem. J.* **265**, 435–452 https://doi.org/10.1042/bj2650435
26 Berrow, N.S., Alderton, D., Sainsbury, S., Nettleship, J., Assenberg, R., Rahman, N. et al. (2007) A versatile ligation-independent cloning method suitable for high-throughput expression screening applications. *Nucleic Acids Res.* **35**, e45 https://doi.org/10.1093/nar/gkm047
27 Whitfield, H., Riley, A.M., Diogenous, S., Godage, H.Y., Potter, B.V.L. and Brearley, C.A. (2018) Simple synthesis of (32)P-labelled inositol hexakisphosphates for study of phosphate transformations. *Plant Soil* **427**, 149–161 https://doi.org/10.1007/s11104-017-3315-9
28 Phillippy, B.Q. and Bland, J.M. (1988) Gradient ion chromatography of inositol phosphates. *Anal. Biochem.* **175**, 162–166 https://doi.org/10.1016/0003-2697(88)90374-0
29 Leatherbarrow, R.J. (2009) *GraFit Version*, 7 edn, Erithacus Software Limited, Horley, U.K
30 Miller, G.J., Wilson, M.P., Majerus, P.W. and Hurley, J.H. (2005) Specificity determinants in inositol polyphosphate synthesis: crystal structure of inositol 1,3,4-trisphosphate 5/6-kinase. *Mol. Cell* **18**, 201–212 https://doi.org/10.1016/j.molcel.2005.03.016
31 Kelley, L.A., Mezulis, S., Yates, C.M., Wass, M.N. and Sternberg, M.J. (2015) The Phyre2 web portal for protein modeling, prediction and analysis. *Nat. Protoc.* **10**, 845–858 https://doi.org/10.1038/nprot.2015.053
32 Emsley, P., Lohkamp, B., Scott, W.G. and Cowtan, K. (2010) Features and development of Coot. *Acta Crystallogr. D Biol. Crystallogr.* **66**, 486–501 https://doi.org/10.1107/S0907444910007493
33 Trott, O. and Olson, A.J. (2010) Autodock Vina: improving the speed and accuracy of docking with a new scoring function, efficient optimization, and multithreading. *J. Comput. Chem.* **31**, 455–461 https://doi.org/10.1002/jcc.21334
34 Ishii, T., Tsuboi, S., Sakane, G., Yamashita, M. and Breedlove, B.K. (2009) Universal spectrochemical series of six-coordinate octahedral metal complexes for modifying the ligand field splitting. *Dalton Trans.* 680–687 https://doi.org/10.1039/B810590A
35 Sommerfeld, V., Kunzel, S., Schollenberger, M., Kuhn, I. and Rodehutscord, M. (2018) Influence of phytase or *myo*-inositol supplements on performance and phytate degradation products in the crop, ileum, and blood of broiler chickens. *Poult. Sci.* **97**, 920–929 https://doi.org/10.3382/ps/pex390
36 Brearley, C.A. and Hanke, D.E. (1996) Inositol phosphates in the duckweed *Spirodela polyrhiza* L. *Biochem. J.* **314** (Pt 1), 215–225 https://doi.org/10.1042/bj3140215
37 Mayr, G.W. (1988) A novel metal-dye detection system permits picomolar-range h.p.l.c. analysis of inositol polyphosphates from non-radioactively labelled cell or tissue specimens. *Biochem. J.* **254**, 585–591 https://doi.org/10.1042/bj2540585
38 Kuo, H.F., Chang, T.Y., Chiang, S.F., Wang, W.D., Charng, Y.Y. and Chiou, T.J. (2014) Arabidopsis inositol pentakisphosphate 2-kinase, AtIPK1, is required for growth and modulates phosphate homeostasis at the transcriptional level. *Plant J.* **80**, 503–515 https://doi.org/10.1111/tpj.12650
39 Shears, S.B., Yang, L. and Qian, X. (2004) Cell signaling by a physiologically reversible inositol phosphate kinase/phosphatase. *Adv. Enzyme Regul.* **44**, 265–277 https://doi.org/10.1016/j.advenzreg.2004.02.002
40 Voglmaier, S.M., Bembenek, M.E., Kaplin, A.I., Dorman, G., Olszewski, J.D., Prestwich, G.D. et al. (1996) Purified inositol hexakisphosphate kinase is an ATP synthase: diphosphoinositol pentakisphosphate as a high-energy phosphate donor. *Proc. Natl. Acad. Sci. U.S.A.* **93**, 4305–4310 https://doi.org/10.1073/pnas.93.9.4305
41 Saiardi, A., Erdjument-Bromage, H., Snowman, A.M., Tempst, P. and Snyder, S.H. (1999) Synthesis of diphosphoinositol pentakisphosphate by a newly identified family of higher inositol polyphosphate kinases. *Curr. Biol.* **9**, 1323–1326 https://doi.org/10.1016/S0960-9822(00)80055-X
42 Shears, S.B. (2015) Inositol pyrophosphates: why so many phosphates? *Adv. Biol. Regul.* **57**, 203–216 https://doi.org/10.1016/j.jbior.2014.09.015
43 Harmel, R.K., Puschmann, R., Nguyen Trung, M., Saiardi, A., Schmieder, P. and Fiedler, D. (2019) Harnessing (13)C-labeled *myo*-inositol to interrogate inositol phosphate messengers by NMR. *Chem. Sci.* **10**, 5267–5274 https://doi.org/10.1039/C9SC00151D
44 Brearley, C.A. and Hanke, D.E. (1996) Inositol phosphates in barley (*Hordeum vulgare* L.) aleurone tissue are stereochemically similar to the products of breakdown of $InsP_6$ *in vitro* by wheat-bran phytase. *Biochem. J.* **318**, 279–286 https://doi.org/10.1042/bj3180279
45 Stephens, L.R., Hawkins, P.T., Stanley, A.F., Moore, T., Poyner, D.R., Morris, P.J. et al. (1991) *myo*-inositol pentakisphosphates. Structure, biological occurrence and phosphorylation to *myo*-inositol hexakisphosphate. *Biochem. J.* **275**, 485–499 https://doi.org/10.1042/bj2750485
46 Brearley, C.A. and Hanke, D.E. (2000) Metabolic relations of inositol 3,4,5,6-tetrakisphosphate revealed by cell permeabilization. Identification of inositol 3,4,5, 6-tetrakisphosphate 1-kinase and inositol 3,4,5,6-tetrakisphosphate phosphatase activities in mesophyll cells. *Plant Physiol.* **122**, 1209–1216 https://doi.org/10.1104/pp.122.4.1209
47 Saiardi, A., Caffrey, J.J., Snyder, S.H. and Shears, S.B. (2000) The inositol hexakisphosphate kinase family. Catalytic flexibility and function in yeast vacuole biogenesis. *J. Biol. Chem.* **275**, 24686–24692 https://doi.org/10.1074/jbc.M002750200
48 Banos-Sanz, J.I., Sanz-Aparicio, J., Whitfield, H., Hamilton, C., Brearley, C.A. and Gonzalez, B. (2012) Conformational changes in inositol 1,3,4,5,6-pentakisphosphate 2-kinase upon substrate binding: role of N-terminal lobe and enantiomeric substrate preference. *J. Biol. Chem.* **287**, 29237–29249 https://doi.org/10.1074/jbc.M112.363671
49 Wundenberg, T., Grabinski, N., Lin, H. and Mayr, G.W. (2014) Discovery of $InsP_6$-kinases as $InsP_6$-dephosphorylating enzymes provides a new mechanism of cytosolic $InsP_6$ degradation driven by the cellular ATP/ADP ratio. *Biochem. J.* **462**, 173–184 https://doi.org/10.1042/BJ20130992
50 Biswas, S., Maity, I.B., Chakrabarti, S. and Biswas, B.B. (1978) Purification and characterization of *myo*-inositol hexaphosphate-adenosine diphosphate phosphotransferase from *Phaseolus aureus*. *Arch. Biochem. Biophys.* **185**, 557–566 https://doi.org/10.1016/0003-9861(78)90201-1

Biochemical Journal (2020) **477** 2621–2638
https://doi.org/10.1042/BCJ20200423

51 Europe-Finner, G.N., Gammon, B. and Newell, P.C. (1991) Accumulation of [^{3}H]-inositol into inositol polyphosphates during development of *Dictyostelium*. *Biochem. Biophys. Res. Commun.* **181**, 191–196 https://doi.org/10.1016/S0006-291X(05)81400-7

52 Stephens, L., Radenberg, T., Thiel, U., Vogel, G., Khoo, K.H., Dell, A. et al. (1993) The detection, purification, structural characterization, and metabolism of diphosphoinositol pentakisphosphate(s) and bisdiphosphoinositol tetrakisphosphate(s). *J. Biol. Chem.* **268**, 4009–4015 PMID: 8440693

53 Menniti, F.S., Miller, R.N., Putney, Jr., J.W. and Shears, S.B. (1993) Turnover of inositol polyphosphate pyrophosphates in pancreatoma cells. *J. Biol. Chem.* **268**, 3850–3856 PMID: 8382679

54 Glennon, M.C. and Shears, S.B. (1993) Turnover of inositol pentakisphosphates, inositol hexakisphosphate and diphosphoinositol polyphosphates in primary cultured hepatocytes. *Biochem. J.* **293**, 583–590 https://doi.org/10.1042/bj2930583

55 Flores, S. and Smart, C.C. (2000) Abscisic acid-induced changes in inositol metabolism in *Spirodela polyrrhiza*. *Planta* **211**, 823–832 https://doi.org/10.1007/s004250000348

56 Dorsch, J.A., Cook, A., Young, K.A., Anderson, J.M., Bauman, A.T., Volkmann, C.J. et al. (2003) Seed phosphorus and inositol phosphate phenotype of barley low phytic acid genotypes. *Phytochemistry* **62**, 691–706 https://doi.org/10.1016/S0031-9422(02)00610-6

57 Burton, A., Hu, X. and Saiardi, A. (2009) Are inositol pyrophosphates signalling molecules? *J. Cell Physiol.* **220**, 8–15 https://doi.org/10.1002/jcp.21763

58 Wilson, M.S., Livermore, T.M. and Saiardi, A. (2013) Inositol pyrophosphates: between signalling and metabolism. *Biochem. J.* **452**, 369–379 https://doi.org/10.1042/BJ20130118

59 Atkinson, D.E. (1968) The energy charge of the adenylate pool as a regulatory parameter. Interaction with feedback modifiers. *Biochemistry* **7**, 4030–4034 https://doi.org/10.1021/bi00851a033

60 De Col, V., Fuchs, P., Nietzel, T., Elsasser, M., Voon, C.P., Candeo, A. et al. (2017) ATP sensing in living plant cells reveals tissue gradients and stress dynamics of energy physiology. *eLife* **6**, e26770 https://doi.org/10.7554/eLife.26770

61 Gout, E., Rebeille, F., Douce, R. and Bligny, R. (2014) Interplay of Mg^{2+}, ADP, and ATP in the cytosol and mitochondria: unravelling the role of Mg^{2+} in cell respiration. *Proc. Natl. Acad. Sci. U.S.A.* **111**, E4560–E4567 https://doi.org/10.1073/pnas.1406251111

62 Voon, C.P., Guan, X., Sun, Y., Sahu, A., Chan, M.N., Gardestrom, P. et al. (2018) ATP compartmentation in plastids and cytosol of *Arabidopsis thaliana* revealed by fluorescent protein sensing. *Proc. Natl. Acad. Sci. U.S.A.* **115**, E10778–E10787 https://doi.org/10.1073/pnas.1711497115

63 Wild, R., Gerasimaite, R., Jung, J.Y., Truffault, V., Pavlovic, I., Schmidt, A. et al. (2016) Control of eukaryotic phosphate homeostasis by inositol polyphosphate sensor domains. *Science* **352**, 986–990 https://doi.org/10.1126/science.aad9858

64 Gu, C., Nguyen, H.N., Hofer, A., Jessen, H.J., Dai, X., Wang, H. et al. (2017) The significance of the bifunctional kinase/phosphatase activities of diphosphoinositol pentakisphosphate kinases (PPIP5Ks) for coupling inositol pyrophosphate cell signaling to cellular phosphate homeostasis. *J. Biol. Chem.* **292**, 4544–4555 https://doi.org/10.1074/jbc.M116.765743

65 Caddick, S.E., Harrison, C.J., Stavridou, I., Mitchell, J.L., Hemmings, A.M. and Brearley, C.A. (2008) A *Solanum tuberosum* inositol phosphate kinase (StITPK1) displaying inositol phosphate-inositol phosphate and inositol phosphate-ADP phosphotransferase activities. *FEBS Lett.* **582**, 1731–1737 https://doi.org/10.1016/j.febslet.2008.04.034

66 Morton, R.K. and Raison, J.K. (1963) A complete intracellular unit for incorporation of amino-acid into storage protein utilizing adenosine triphosphate generated from phytate. *Nature* **200**, 429–433 https://doi.org/10.1038/200429a0

67 Desfougeres, Y., Wilson, M.S.C., Laha, D., Miller, G.J. and Saiardi, A. (2019) ITPK1 mediates the lipid-independent synthesis of inositol phosphates controlled by metabolism. *Proc. Natl. Acad. Sci. U.S.A.* **116**, 24551–24561 https://doi.org/10.1073/pnas.1911431116

68 Alexova, R., Nelson, C.J. and Millar, A.H. (2017) Temporal development of the barley leaf metabolic response to Pi limitation. *Plant Cell Environ.* **40**, 645–657 https://doi.org/10.1111/pce.12882